A Novel, Cost-Effective, High-Channel-Density Multi-point Thomson Scattering System for Diagnosing High-Temperature Plasmas on the Pegasus Toroidal Experiment

D.J. Schlossberg

J.L. Barr, G.M. Bodner, M.W. Bongard, M.G. Burke,
R.J. Fonck, J.M. Perry, J.A. Reusch, C. Rodriguez Sanchez

21st Topical Conference on High-Temperature Plasma Diagnostics
June 5-9, 2016
Madison, WI

Motivation

- Pegasus system takes pragmatic approach to Thomson scattering:
  - Design for simplicity, low personnel-requirements, cost-effectiveness
  - Accept some cost to total efficiency





Motivation

- Pegasus system takes pragmatic approach to Thomson scattering:
  - Design for simplicity, low personnel-requirements, cost-effectiveness
  - Accept some cost to total efficiency

- Result: a highly-optimized system





Motivation

- Pegasus system takes pragmatic approach to Thomson scattering:
  - Design for simplicity, low personnel-requirements, cost-effectiveness
  - Accept some cost to total efficiency

- Result: a highly-optimized system
  - Detectors use image-intensifiers with increased efficiency 400 – 700 nm
  - Diffraction gratings optimized for this wavelength range
  - Frequency-doubled Nd:YAG laser (532 nm) emits in center of this range





Motivation

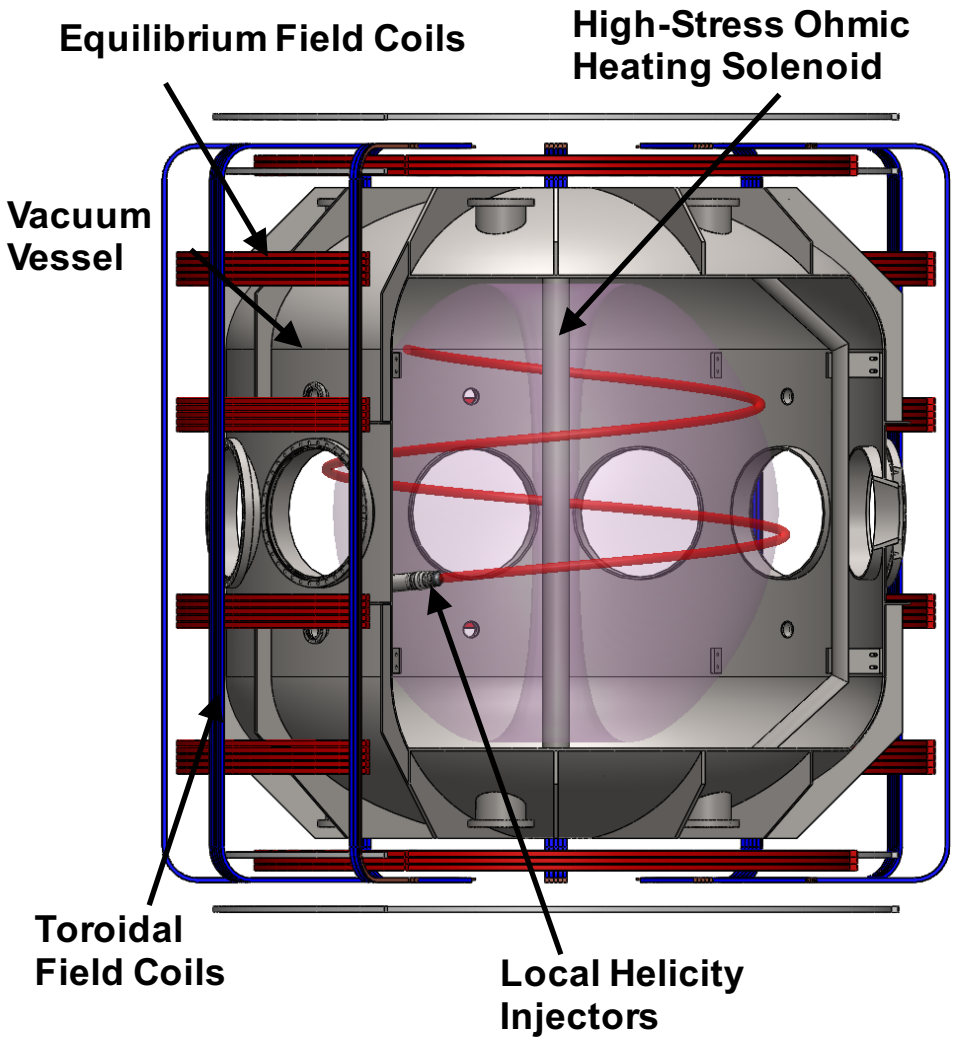
- Pegasus system takes pragmatic approach to Thomson scattering:
  - Design for simplicity, low personnel-requirements, cost-effectiveness
  - Accept some cost to total efficiency

- Result: a highly-optimized system
  - Detectors use image-intensifiers with increased efficiency 400 – 700 nm
  - Diffraction gratings optimized for this wavelength range
  - Frequency-doubled Nd:YAG laser (532 nm) emits in center of this range
  - Image intensifiers provide time-of-flight stray light rejection
  - Easily reconfigurable wavelength bins
  - Low maintenance with fully automated intra-shot laser alignment





Pegasus is a compact, ultralow aspect ratio spherical tokamak



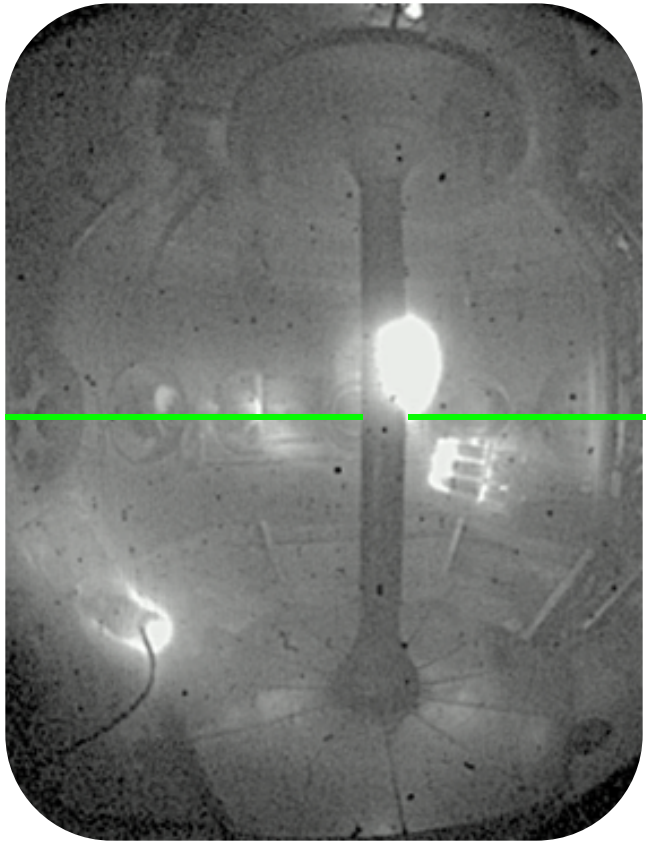
Experimental Parameters

Parameter	Achieved
A	1.15 – 1.3
R(m)	0.2 – 0.45
I_p (MA)	≤ .21
κ	1.4 – 3.7
τ_{shot} (s)	≤ 0.025
β_t (%)	≤ 25

Major research thrusts include:

- *Non-inductive startup and sustainment*
- *Plasma stability as A → 1*

Plasma and Thomson sightline



A novel Thomson scattering system was conceptualized, designed and implemented

- Guiding principles for Pegasus design:
  1. Simplicity
  2. Cost-effectiveness
  3. Ease of expansion





A novel Thomson scattering system was conceptualized, designed and implemented

- Guiding principles for Pegasus design:
  1. Simplicity
  2. Cost-effectiveness
  3. Ease of expansion

Parameter	Value
Expected e- temperatures	10 – 1000 eV
Typical densities	0.1 – 5 x 10^{19} m^{-3}
Major radius viewing range	11 – 85 cm
Scattering length/channel	1.2 cm
Spatial channels	24
Spatial channels/spectrometer	8
System etendue	0.87 mm^2-ster
Collection f/# (on-axis)	6
Laser wavelength	532 nm
Laser pulse energy	>2.0 J
Number of laser photons/pulse	5 x 10^{18}
Photo-electrons/10^{19} plasma e-	≈4.8 x 10^3

A novel Thomson scattering system was conceptualized, designed and implemented

- Guiding principles for Pegasus design:
  1. Simplicity
  2. Cost-effectiveness
  3. Ease of expansion

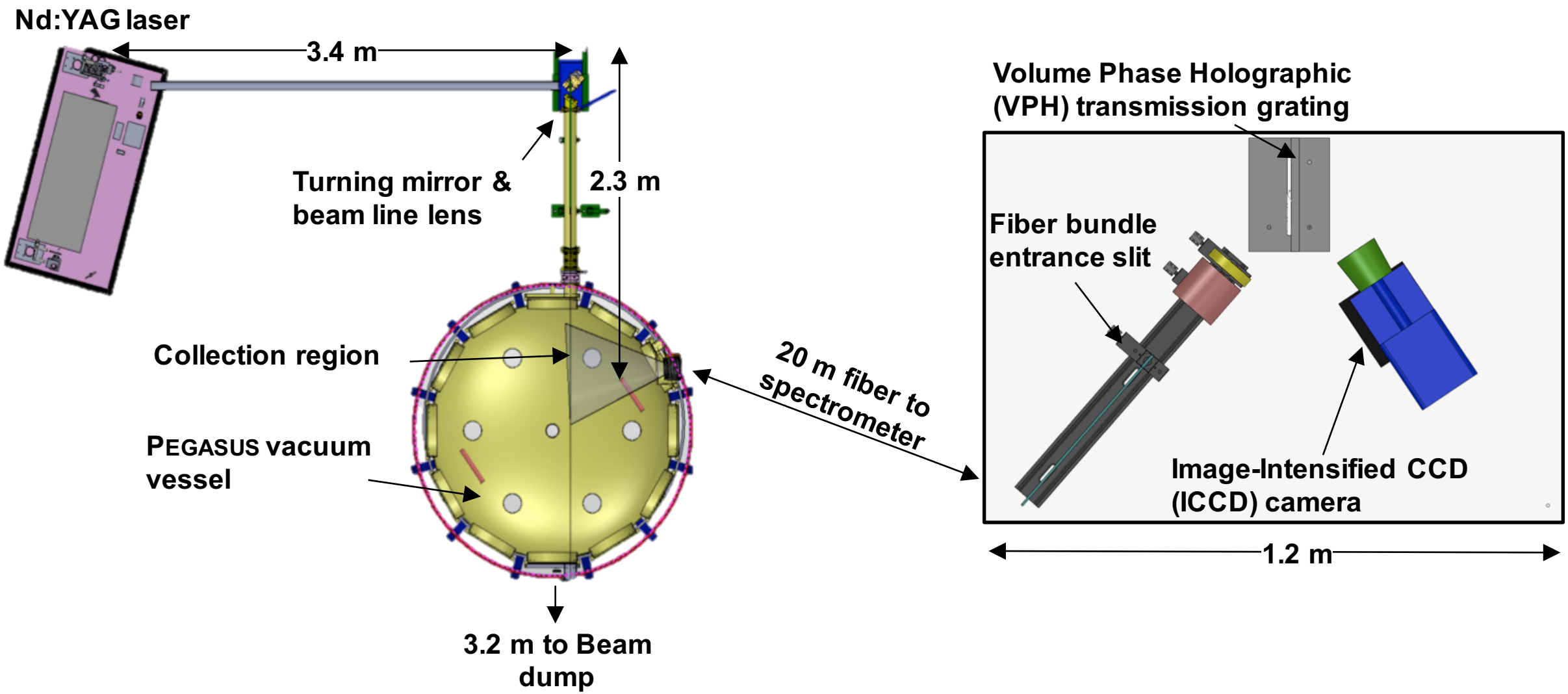
- These criteria led to unique design choices

Parameter	Value
Expected e- temperatures	10 – 1000 eV
Typical densities	0.1 – 5 x 10^{19} m^{-3}
Major radius viewing range	11 – 85 cm
Scattering length/channel	1.2 cm
Spatial channels	24
Spatial channels/spectrometer	8
System etendue	0.87 mm^2-ster
Collection f/# (on-axis)	6
Laser wavelength	532 nm
Laser pulse energy	>2.0 J
Number of laser photons/pulse	5 x 10^{18}
Photo-electrons/10^{19} plasma e-	≈4.8 x 10^3



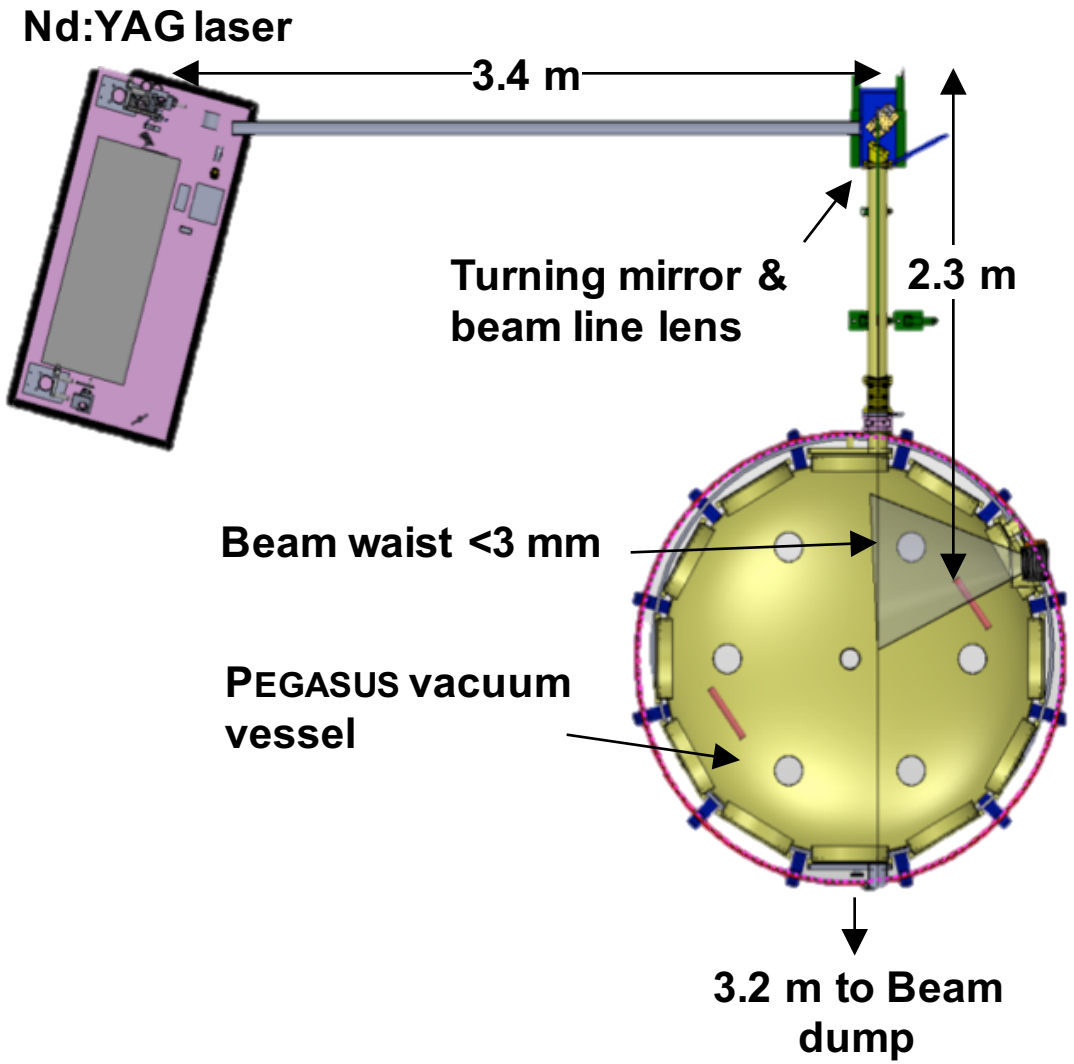


Pegasus Thomson scattering uses Nd:YAG laser at 532 nm, transmission gratings, and ICCD cameras



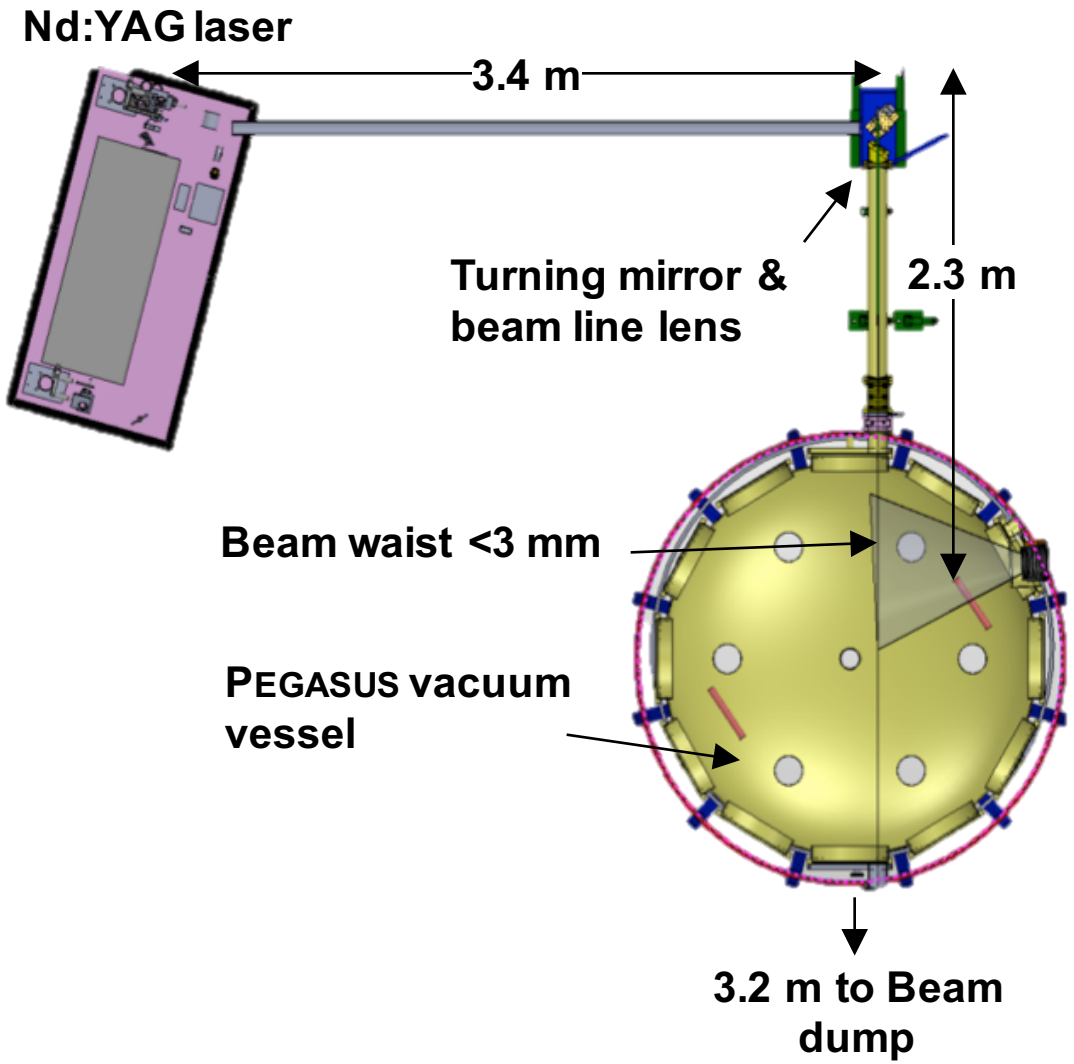
For more information, see:
D.J. Schlossberg, Rev. Sci. Instrum. ***83****, 10E335 (2012).*
D.J. Schlossberg, J. Instrumentation, ***8****, 11, C11019 (2013).*

Nd:YAG laser at 532 nm provides 2 J at 10 Hz



For more information, see:
D.J. Schlossberg, Rev. Sci. Instrum. ***83****, 10E335 (2012).*
D.J. Schlossberg, J. Instrumentation, ***8****, 11, C11019 (2013).*

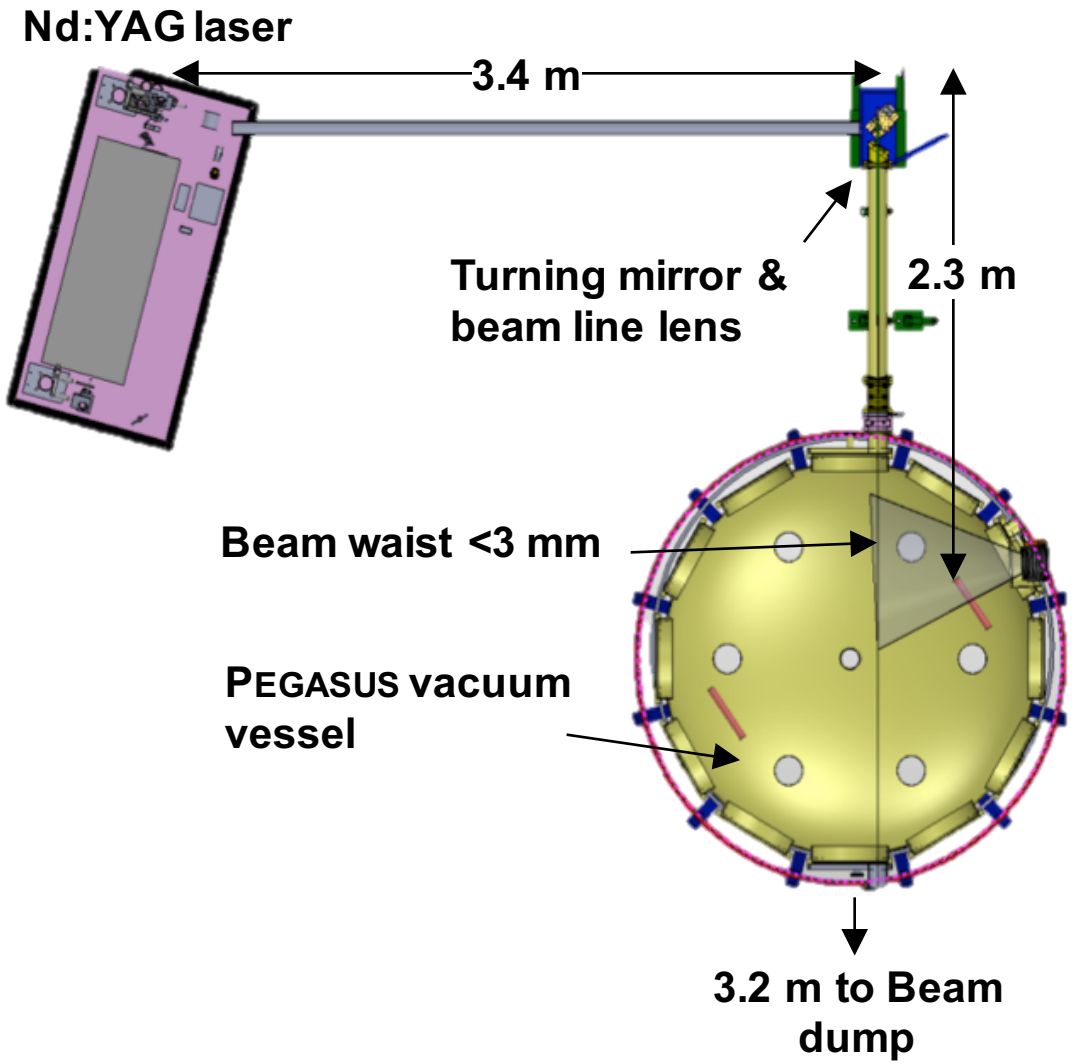
Nd:YAG laser at 532 nm provides 2 J at 10 Hz



- Commercial laser:
  Continuum Powerlite DLS Plus 2 J
- Reliable, "turn-key" operation of laser desired
  - Low impact on personnel requirements

For more information, see:
D.J. Schlossberg, Rev. Sci. Instrum. ***83****, 10E335 (2012).*
D.J. Schlossberg, J. Instrumentation, ***8****, 11, C11019 (2013).*

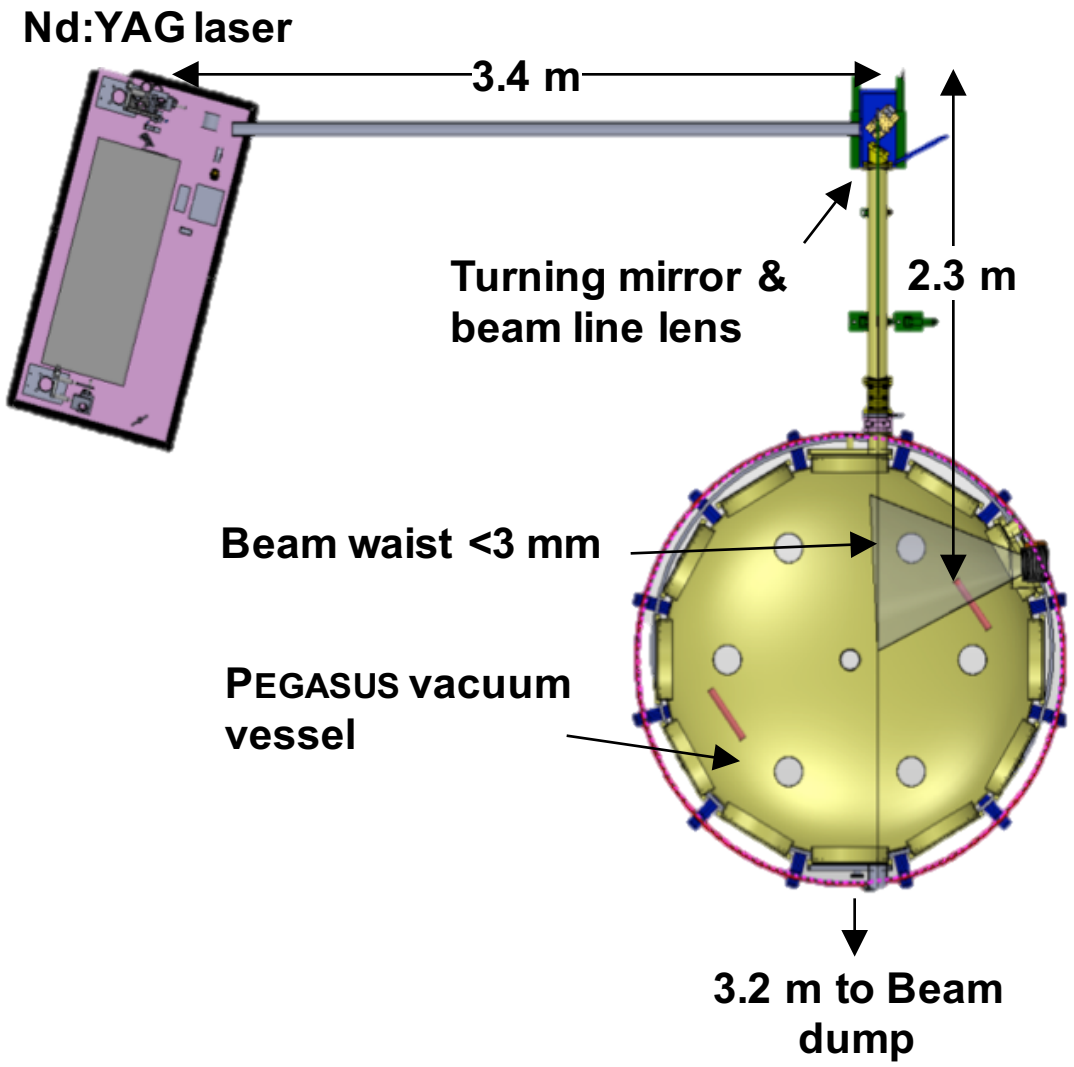
Nd:YAG laser at 532 nm provides 2 J at 10 Hz



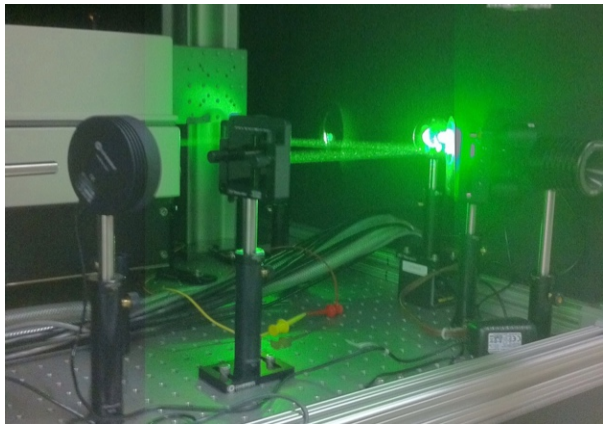
- Commercial laser:
  Continuum Powerlite DLS Plus 2 J
- Reliable, "turn-key" operation of laser desired
  - Low impact on personnel requirements
- Operate at 2ω to match peak sensitivity of detectors

For more information, see:
D.J. Schlossberg, Rev. Sci. Instrum. ***83****, 10E335 (2012).*
D.J. Schlossberg, J. Instrumentation, ***8****, 11, C11019 (2013).*

Nd:YAG laser at 532 nm provides 2 J at 10 Hz

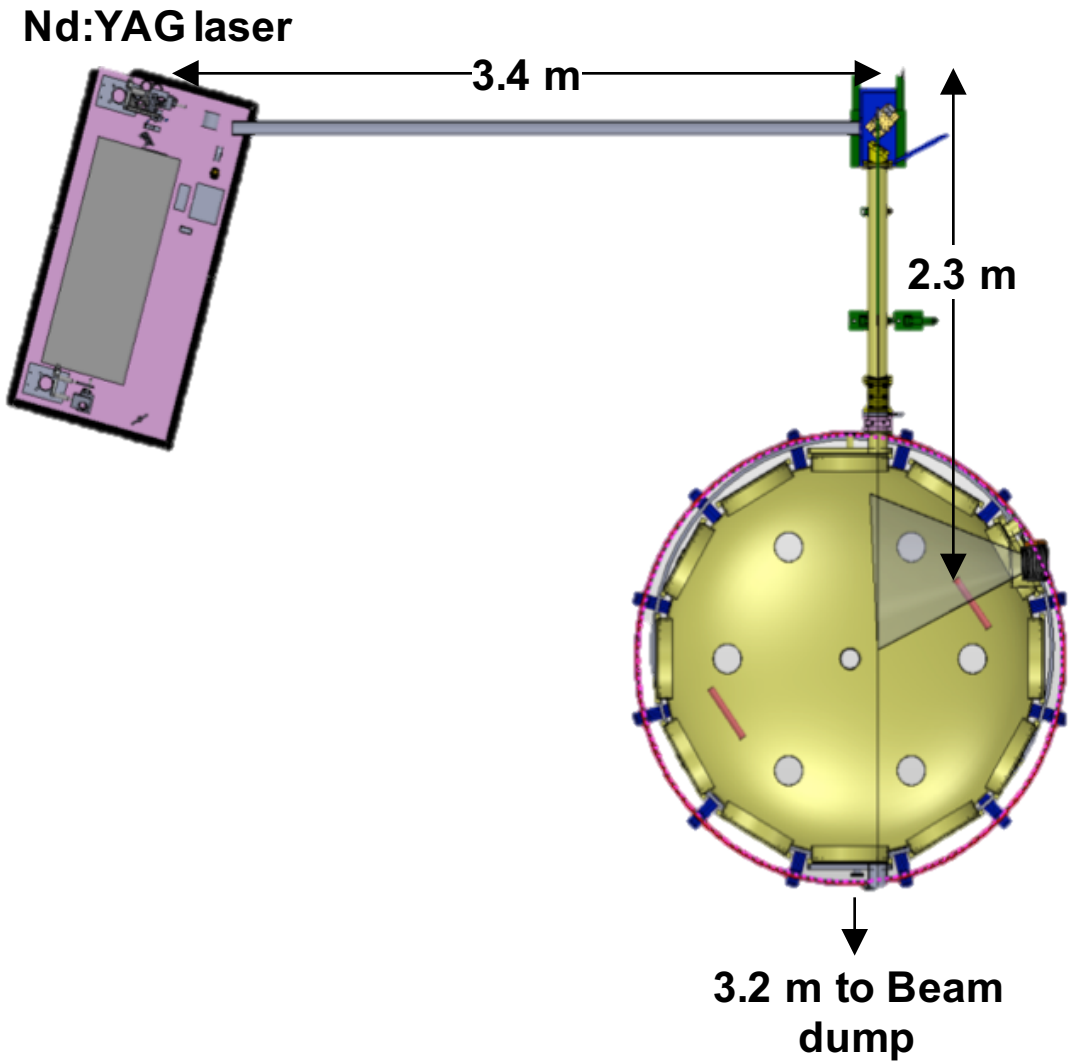


- Commercial laser: Continuum Powerlite DLS Plus 2 J
- Reliable, "turn-key" operation of laser desired
  - Low impact on personnel requirements
- Operate at 2ω to match peak sensitivity of detectors
- Visible lasing eases alignment and safety issues



For more information, see:
D.J. Schlossberg, Rev. Sci. Instrum. ***83****, 10E335 (2012).*
D.J. Schlossberg, J. Instrumentation, ***8****, 11, C11019 (2013).*

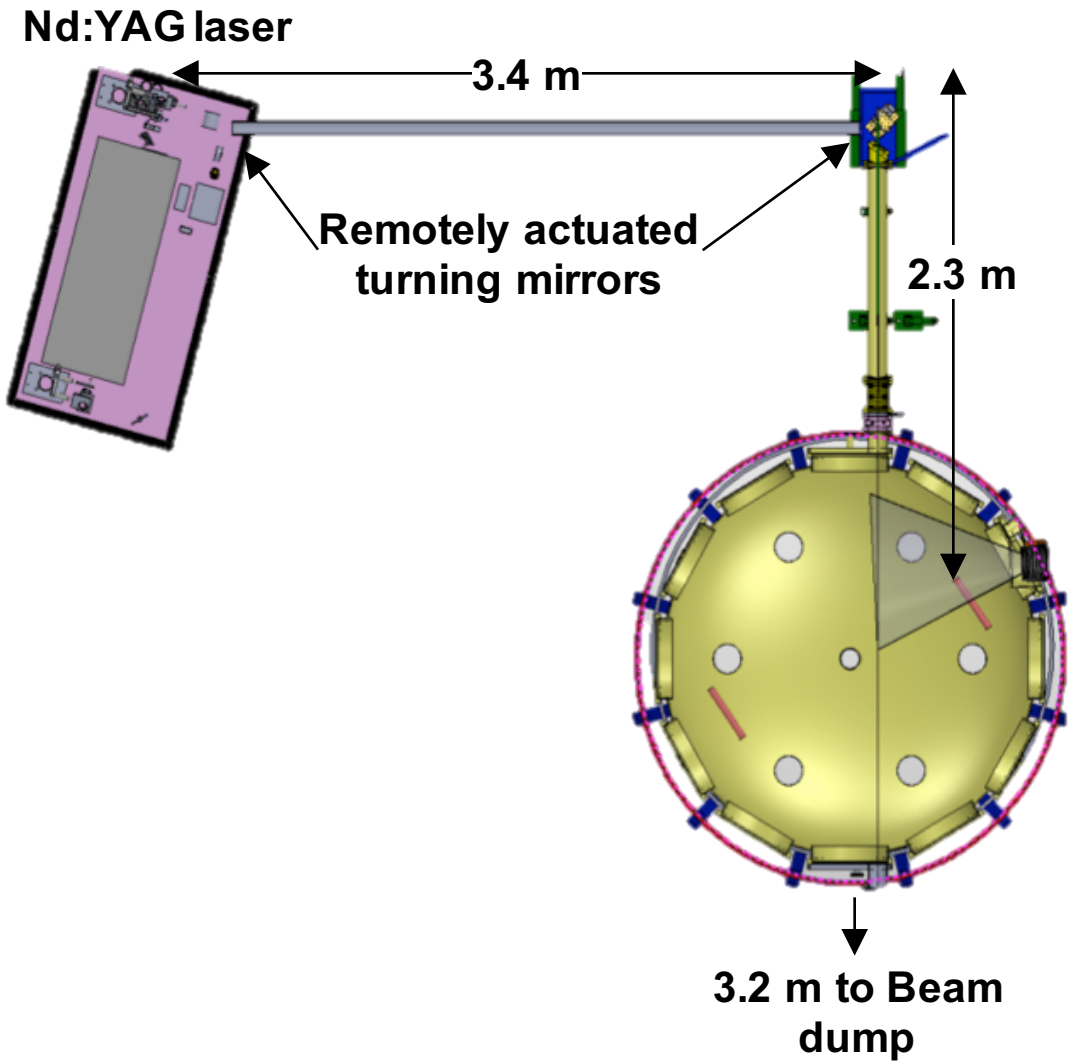
Laser system features intra-shot, automated alignment



- Alignment uses precision, off-the-shelf components
  - Remotely actuated turning mirrors, 11.1μm adjustment
  - Ethernet-based cameras monitor beam entrance & exit

See poster next session, Grant Bodner 6.2.09

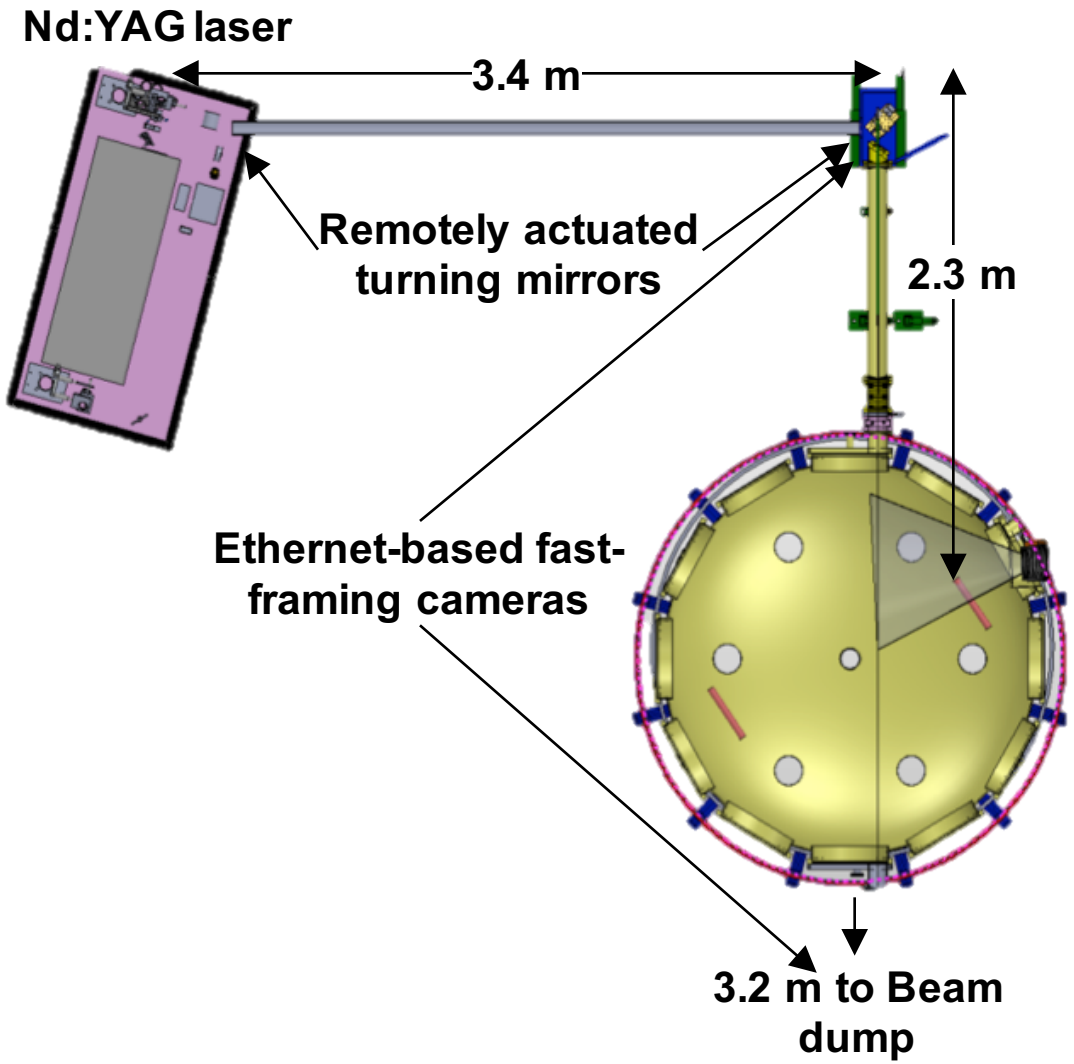
Laser system features intra-shot, automated alignment



- Alignment uses precision, off-the-shelf components
  - Remotely actuated turning mirrors, 11.1μm adjustment
  - Ethernet-based cameras monitor beam entrance & exit

See poster next session, Grant Bodner 6.2.09

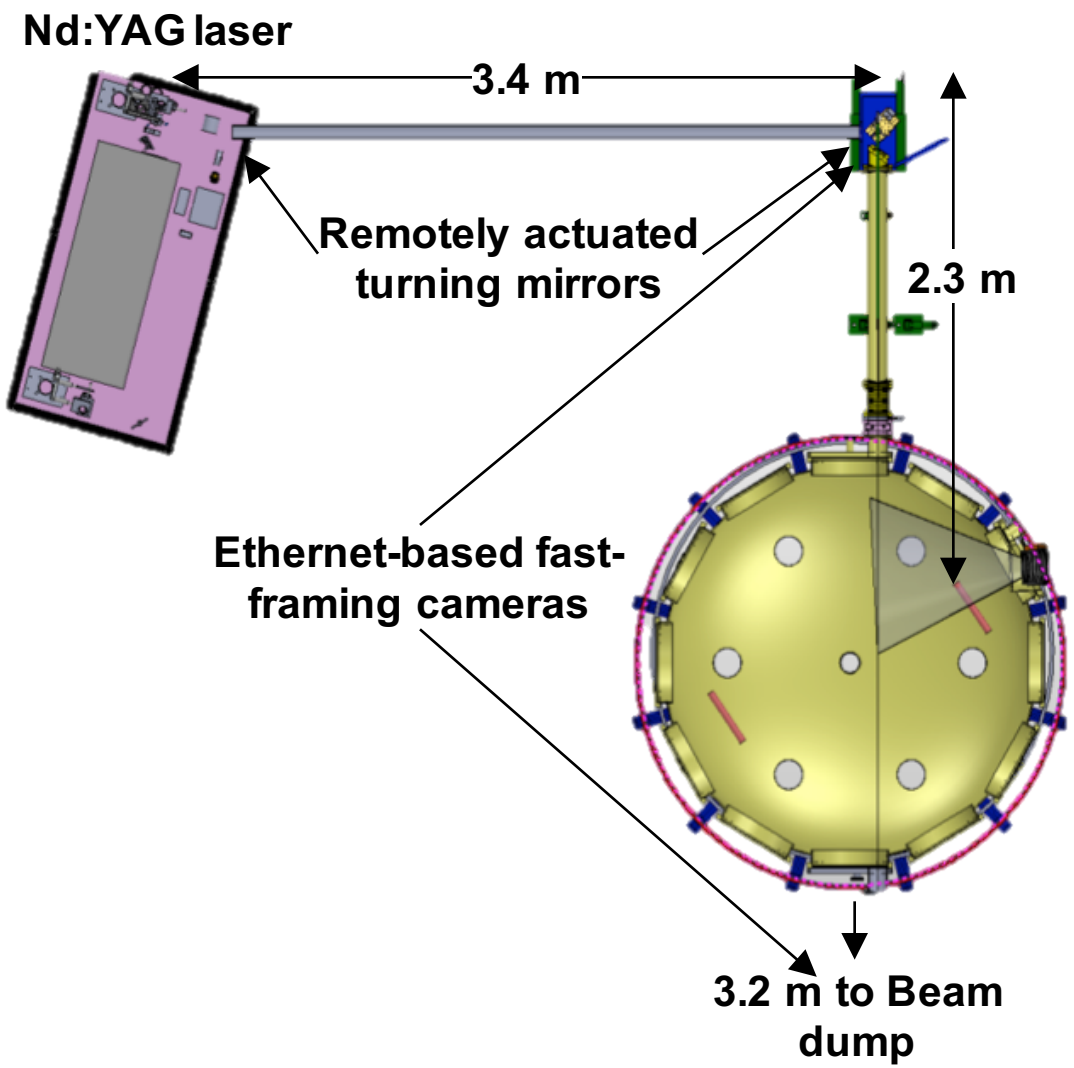
Laser system features intra-shot, automated alignment



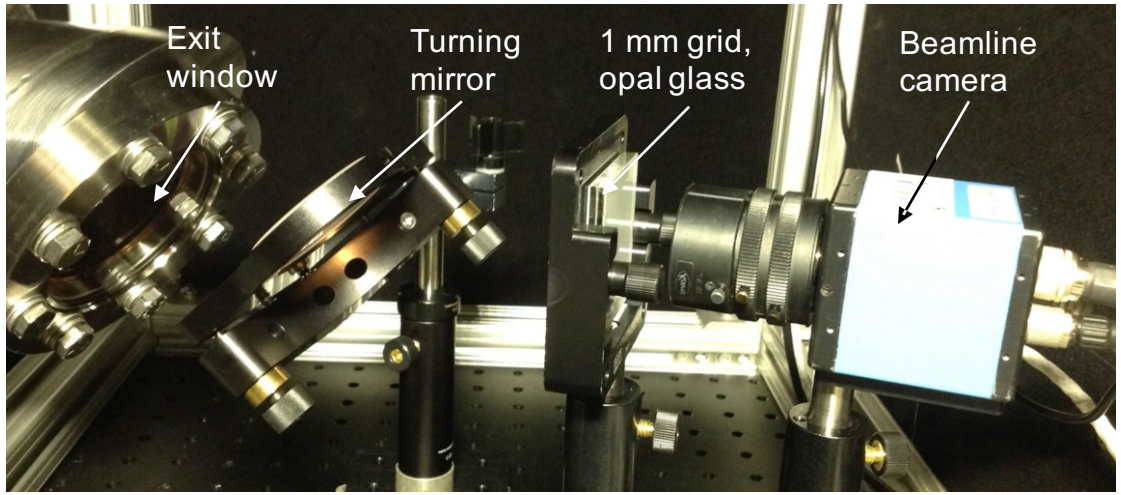
- Alignment uses precision, off-the-shelf components
  - Remotely actuated turning mirrors, 11.1μm adjustment
  - Ethernet-based cameras monitor beam entrance & exit

See poster next session, Grant Bodner 6.2.09

Laser system features intra-shot, automated alignment

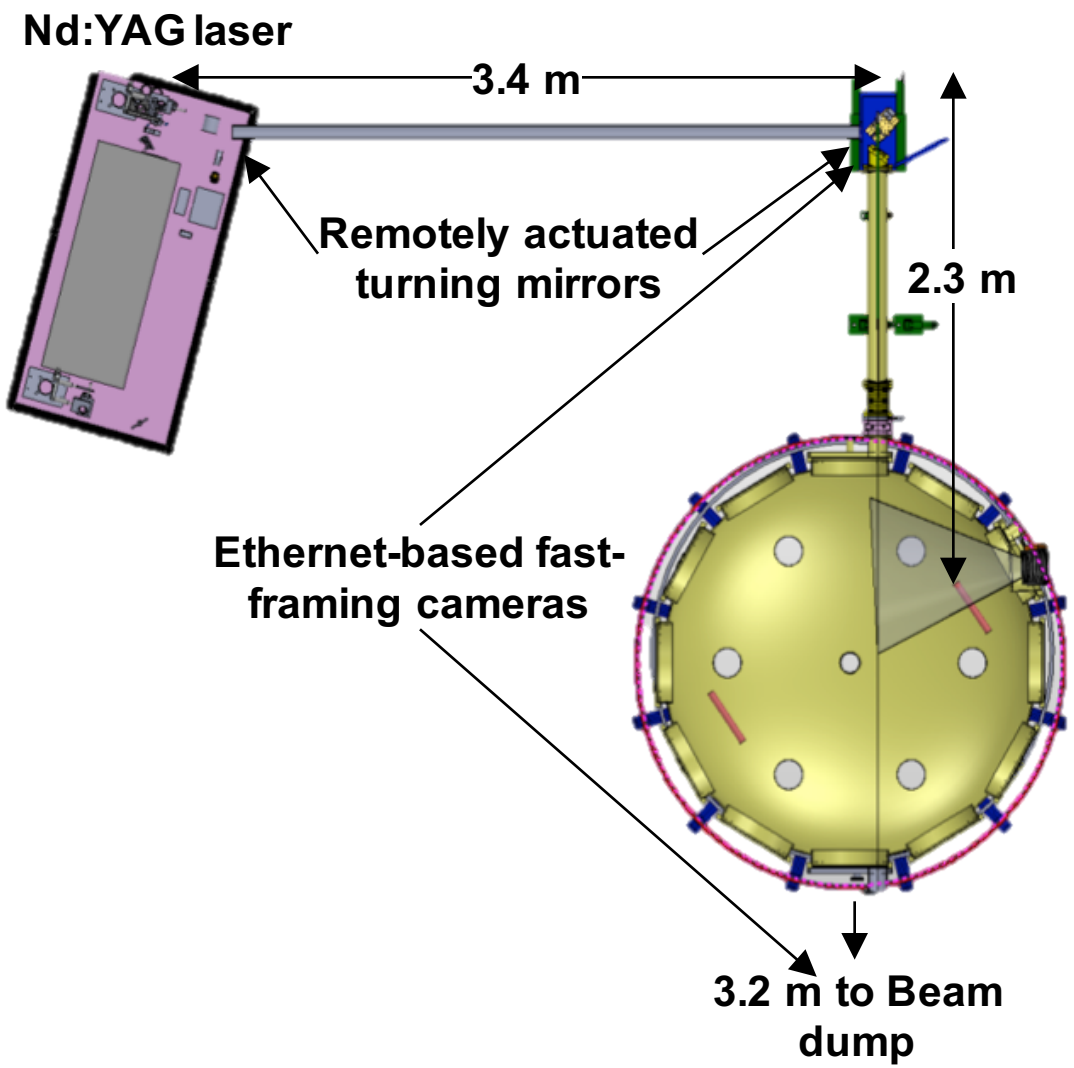


- Alignment uses precision, off-the-shelf components
  - Remotely actuated turning mirrors, 11.1μm adjustment
  - Ethernet-based cameras monitor beam entrance & exit

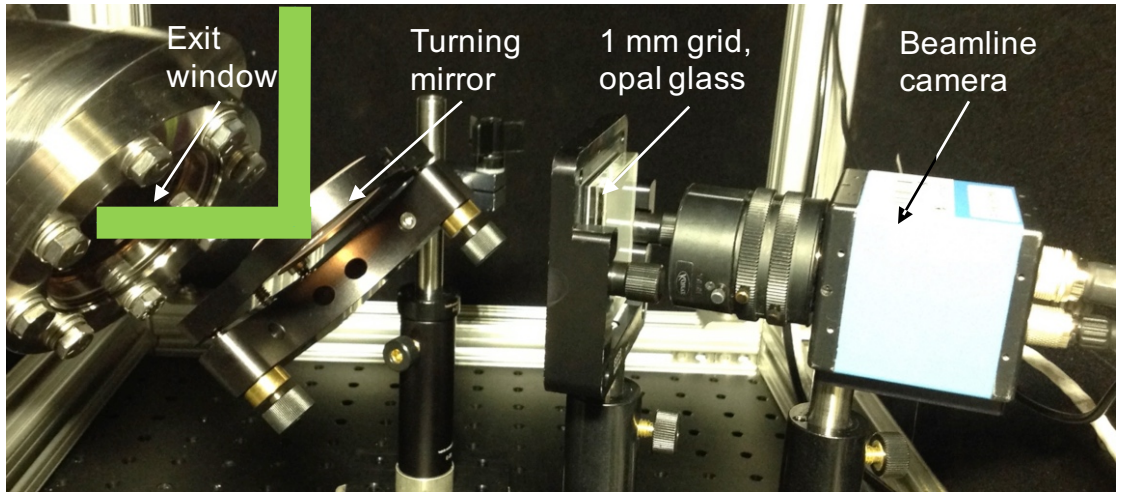


See poster next session, Grant Bodner 6.2.09

Laser system features intra-shot, automated alignment

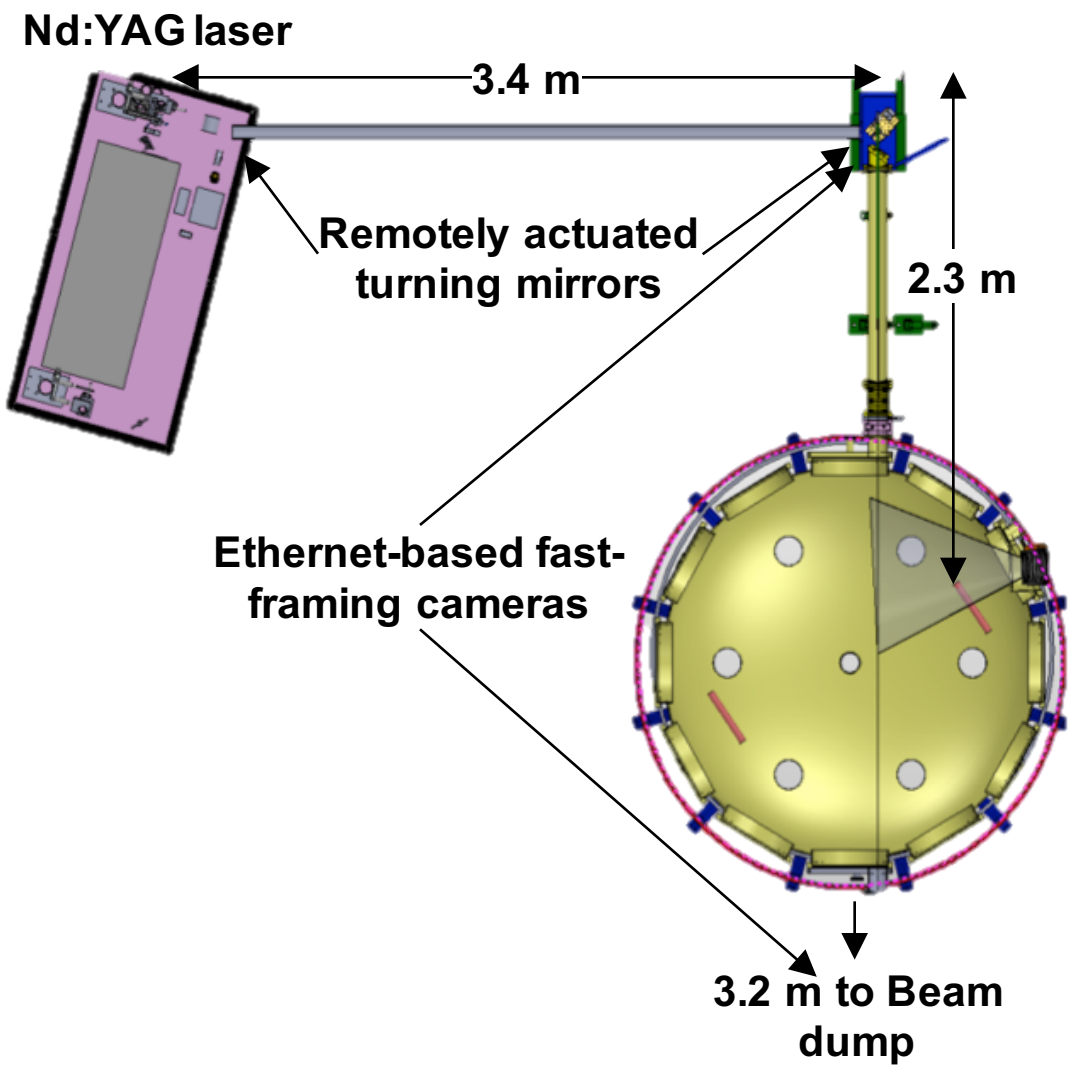


- Alignment uses precision, off-the-shelf components
  - Remotely actuated turning mirrors, 11.1μm adjustment
  - Ethernet-based cameras monitor beam entrance & exit

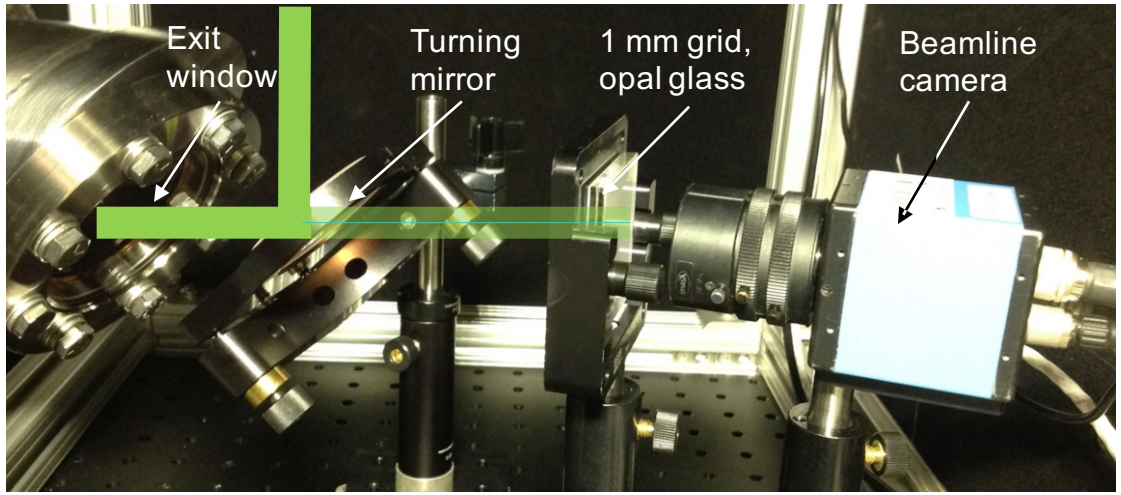


See poster next session, Grant Bodner 6.2.09

Laser system features intra-shot, automated alignment

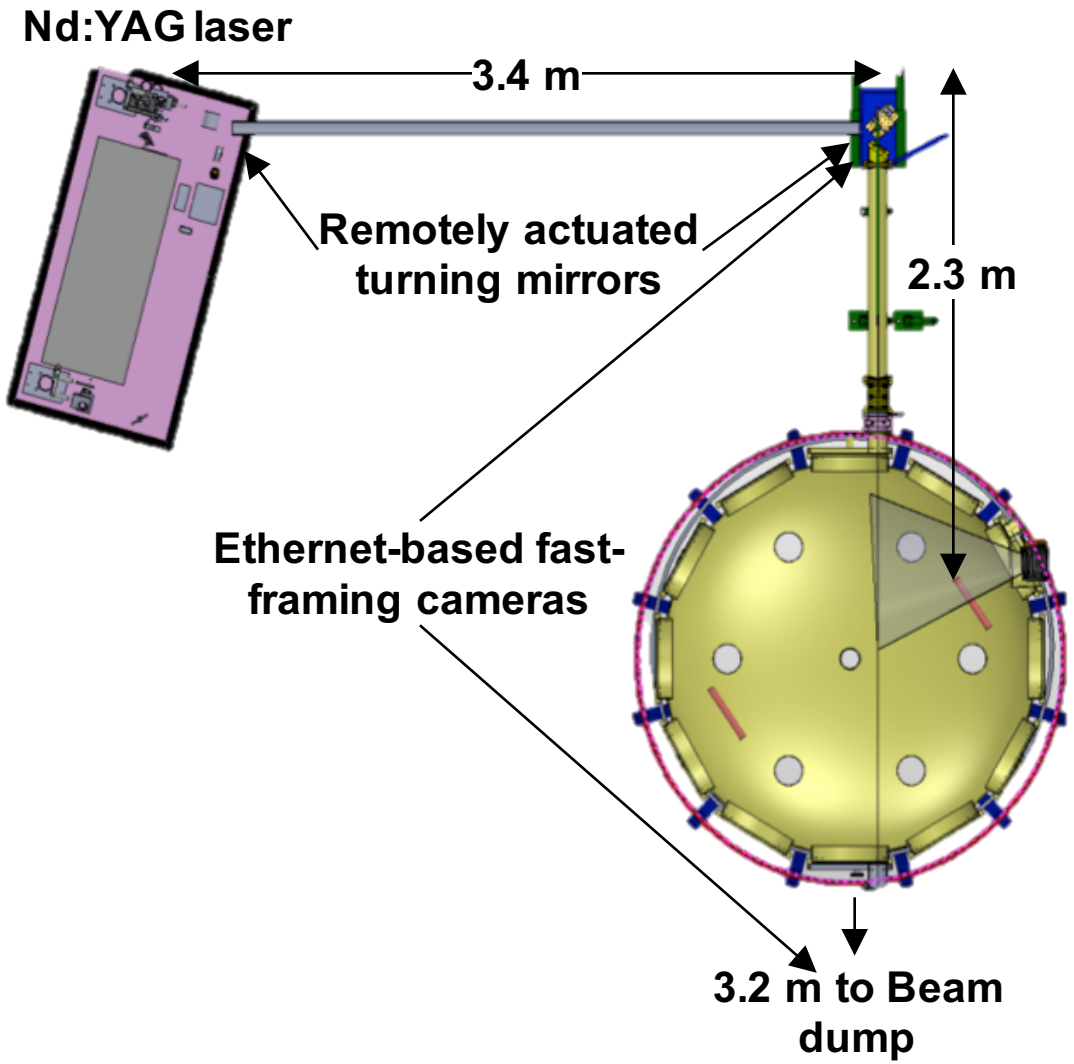


- Alignment uses precision, off-the-shelf components
  - Remotely actuated turning mirrors, 11.1μm adjustment
  - Ethernet-based cameras monitor beam entrance & exit
  - Beam is attenuated through mirror, then ND filter stack



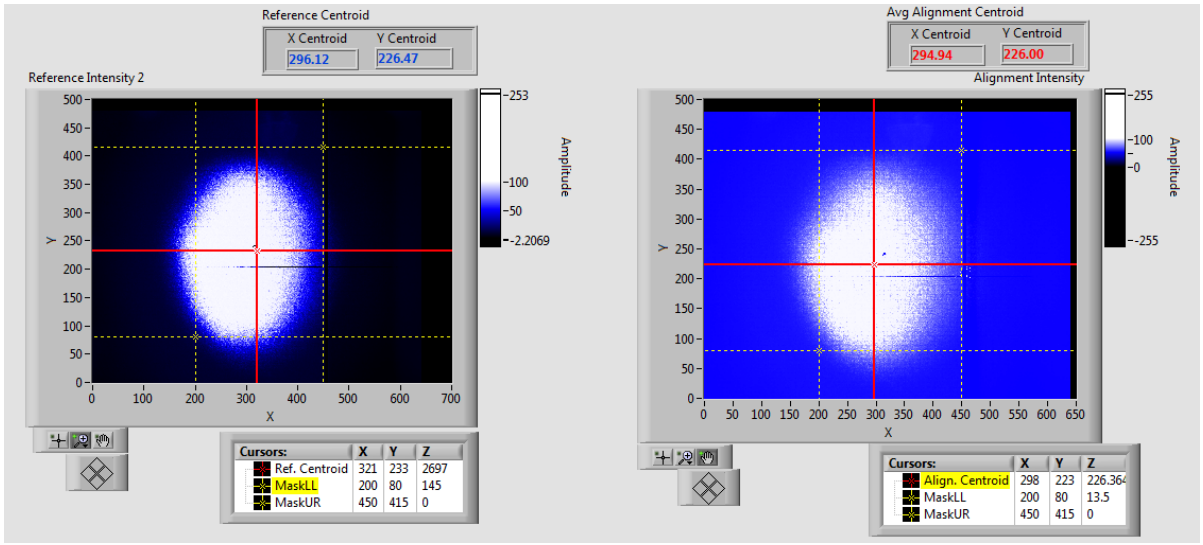
See poster next session, Grant Bodner 6.2.09

Laser system features intra-shot, automated alignment



- Alignment uses precision, off-the-shelf components
  - Remotely actuated turning mirrors, 11.1μm adjustment
  - Ethernet-based cameras monitor beam entrance & exit
  - Beam is attenuated through mirror, then ND filter stack

- LabVIEW routine feeds back on image centroids to automatically align laser



See poster next session, Grant Bodner 6.2.09

Spectrometers employ VPH gratings and ICCD cameras: High efficiency in visible region

For more information, see:
N.L. Schoenbeck, et al. Rev. Sci. Instrum. ***83****, 10E330 (2012)*

Spectrometers employ VPH gratings and ICCD cameras: High efficiency in visible region

- For expected T_e, scattering from $532 < \lambda < 600$ nm

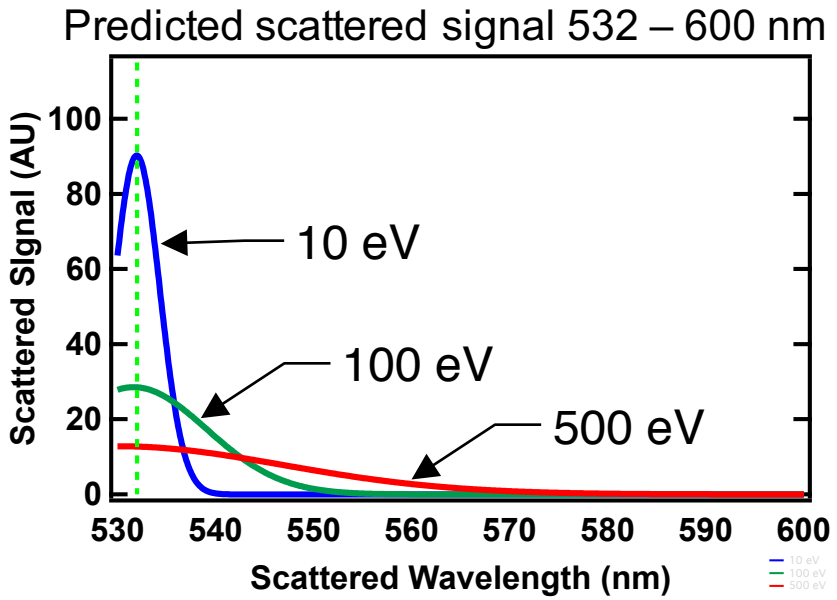


For more information, see:
N.L. Schoenbeck, et al. Rev. Sci. Instrum. ***83****, 10E330 (2012)*



Spectrometers employ VPH gratings and ICCD cameras: High efficiency in visible region

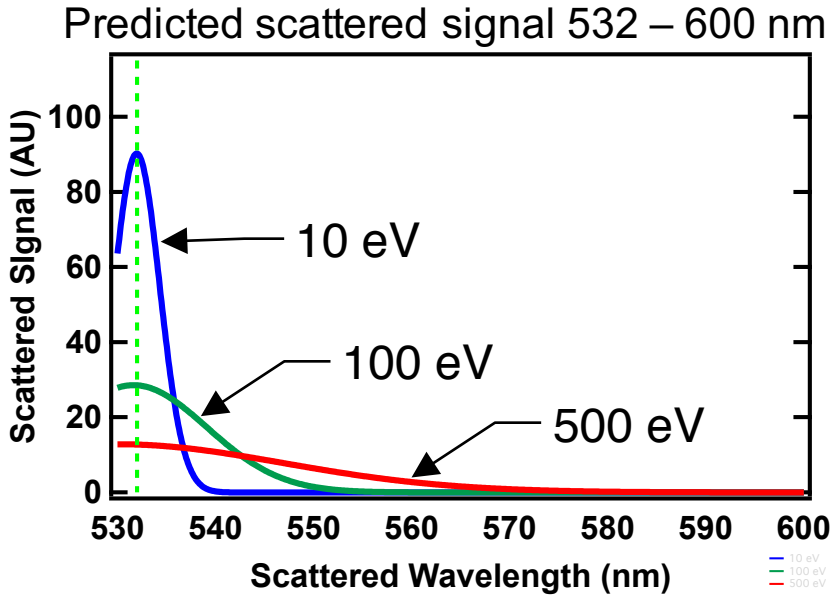
- For expected T_e, scattering from $532 < \lambda < 600$ nm



For more information, see:
N.L. Schoenbeck, et al. Rev. Sci. Instrum. ***83****, 10E330 (2012)*

Spectrometers employ VPH gratings and ICCD cameras: High efficiency in visible region

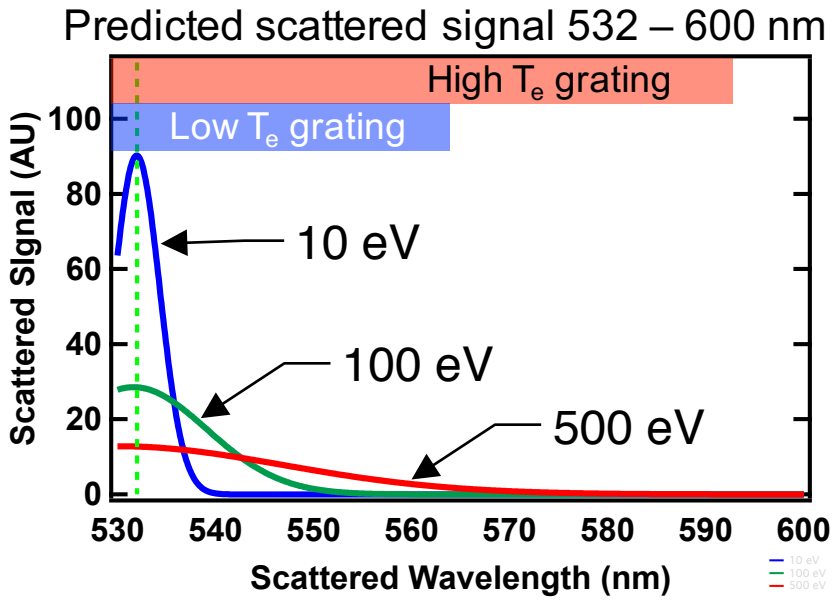
- For expected T_e, scattering from $532 < \lambda < 600$ nm
- Divide into 2 regions for optimized resolution
  - Use 2 gratings with interchangeable, kinematic mounts



For more information, see:
N.L. Schoenbeck, et al. Rev. Sci. Instrum. ***83****, 10E330 (2012)*

Spectrometers employ VPH gratings and ICCD cameras: High efficiency in visible region

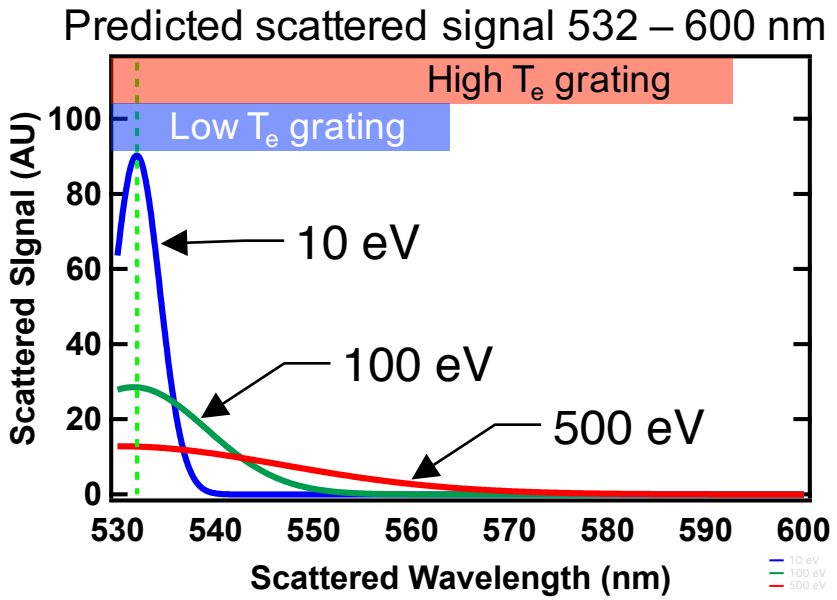
- For expected T_e, scattering from $532 < \lambda < 600$ nm
- Divide into 2 regions for optimized resolution
  - Use 2 gratings with interchangeable, kinematic mounts



For more information, see:
N.L. Schoenbeck, et al. Rev. Sci. Instrum. ***83****, 10E330 (2012)*

Spectrometers employ VPH gratings and ICCD cameras: High efficiency in visible region

- For expected T_e, scattering from $532 < \lambda < 600$ nm
- Divide into 2 regions for optimized resolution
  - Use 2 gratings with interchangeable, kinematic mounts
  - Optimize diffraction efficiency for each range

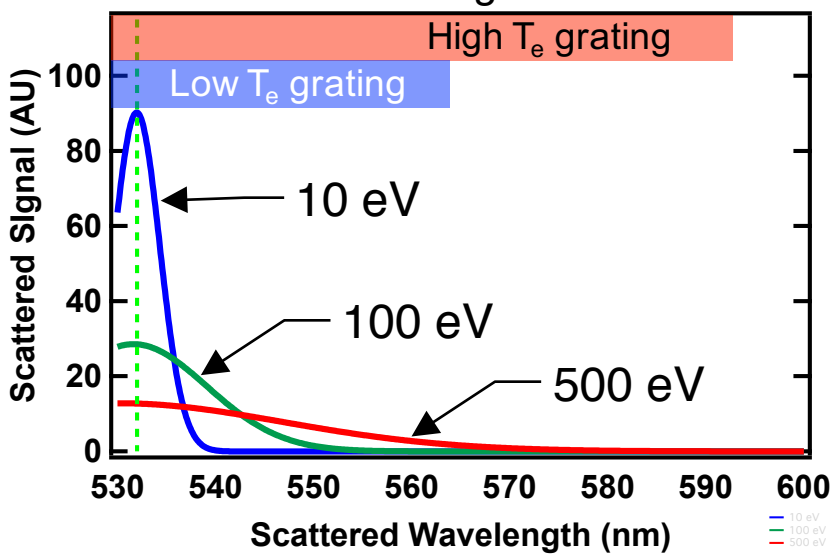


For more information, see:
N.L. Schoenbeck, et al. Rev. Sci. Instrum. ***83****, 10E330 (2012)*

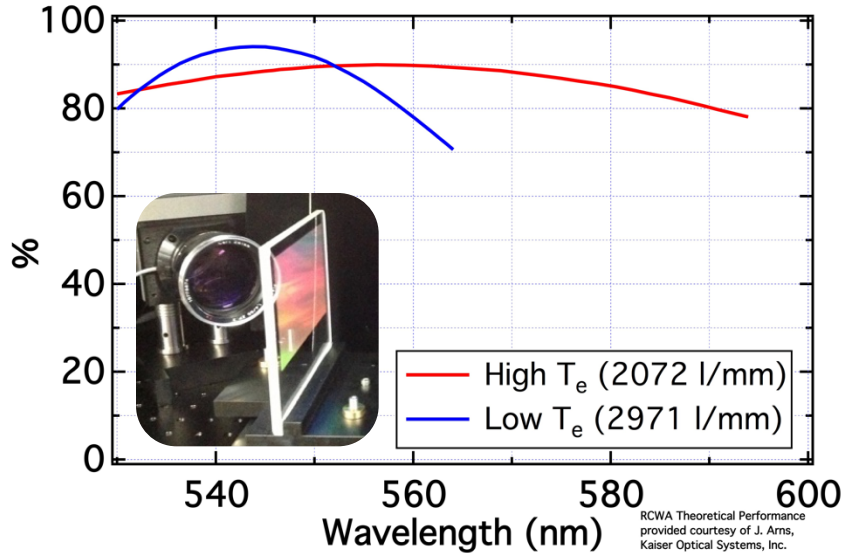
Spectrometers employ VPH gratings and ICCD cameras: High efficiency in visible region

- For expected T_e, scattering from $532 < \lambda < 600$ nm
- Divide into 2 regions for optimized resolution
  - Use 2 gratings with interchangeable, kinematic mounts
  - Optimize diffraction efficiency for each range

Predicted scattered signal 532 – 600 nm



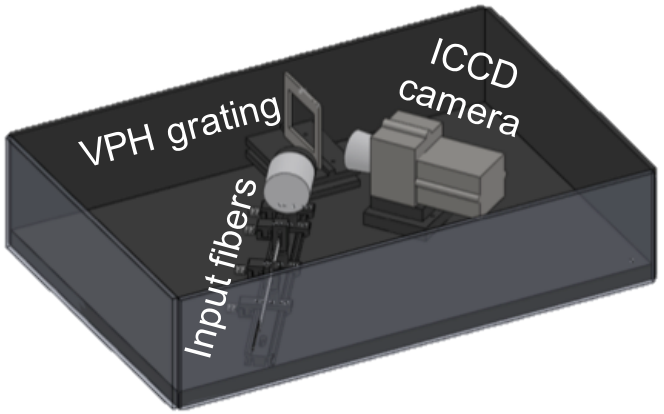
Optimized diffraction efficiency for 2 gratings



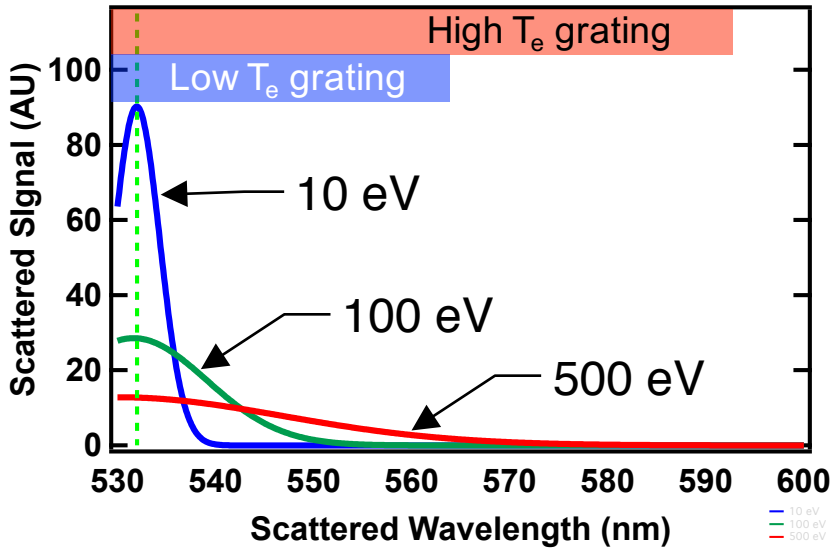
For more information, see:
N.L. Schoenbeck, et al. Rev. Sci. Instrum. ***83****, 10E330 (2012)*

Spectrometers employ VPH gratings and ICCD cameras: High efficiency in visible region

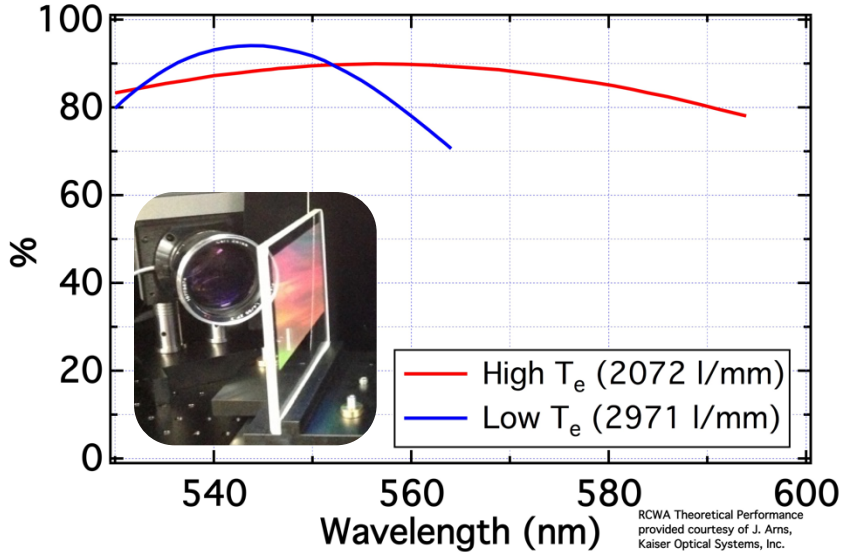
- For expected T_e, scattering from $532 < \lambda < 600$ nm
- Divide into 2 regions for optimized resolution
  - Use 2 gratings with interchangeable, kinematic mounts
  - Optimize diffraction efficiency for each range
- Detector is an Image Intensified CCD (ICCD) camera
  - Generation 3 photocathode with QE ~ 50%
  - Fast gating capability to 1.2 ns



Predicted scattered signal 532 – 600 nm



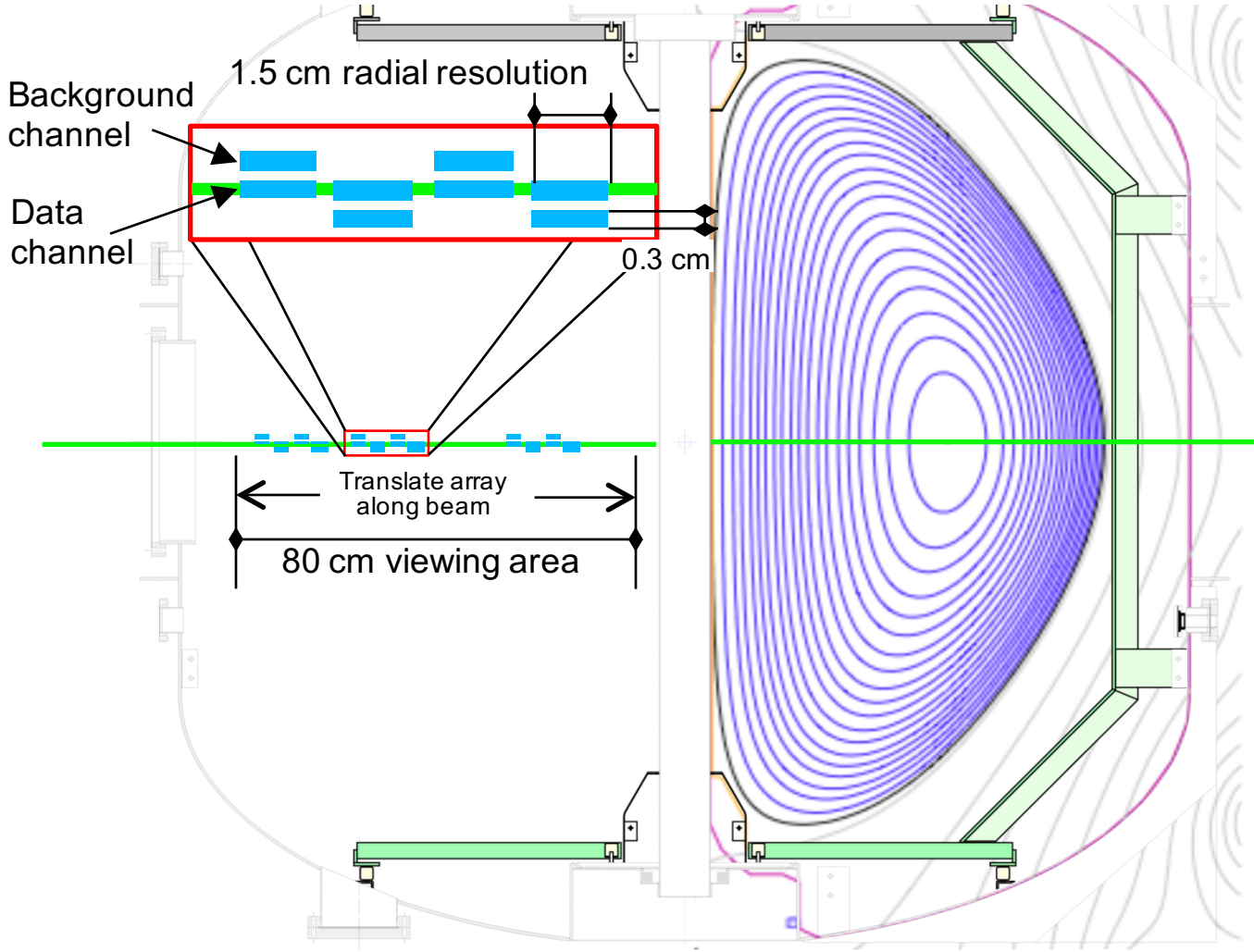
Optimized diffraction efficiency for 2 gratings



For more information, see:
N.L. Schoenbeck, et al. Rev. Sci. Instrum. ***83****, 10E330 (2012)*

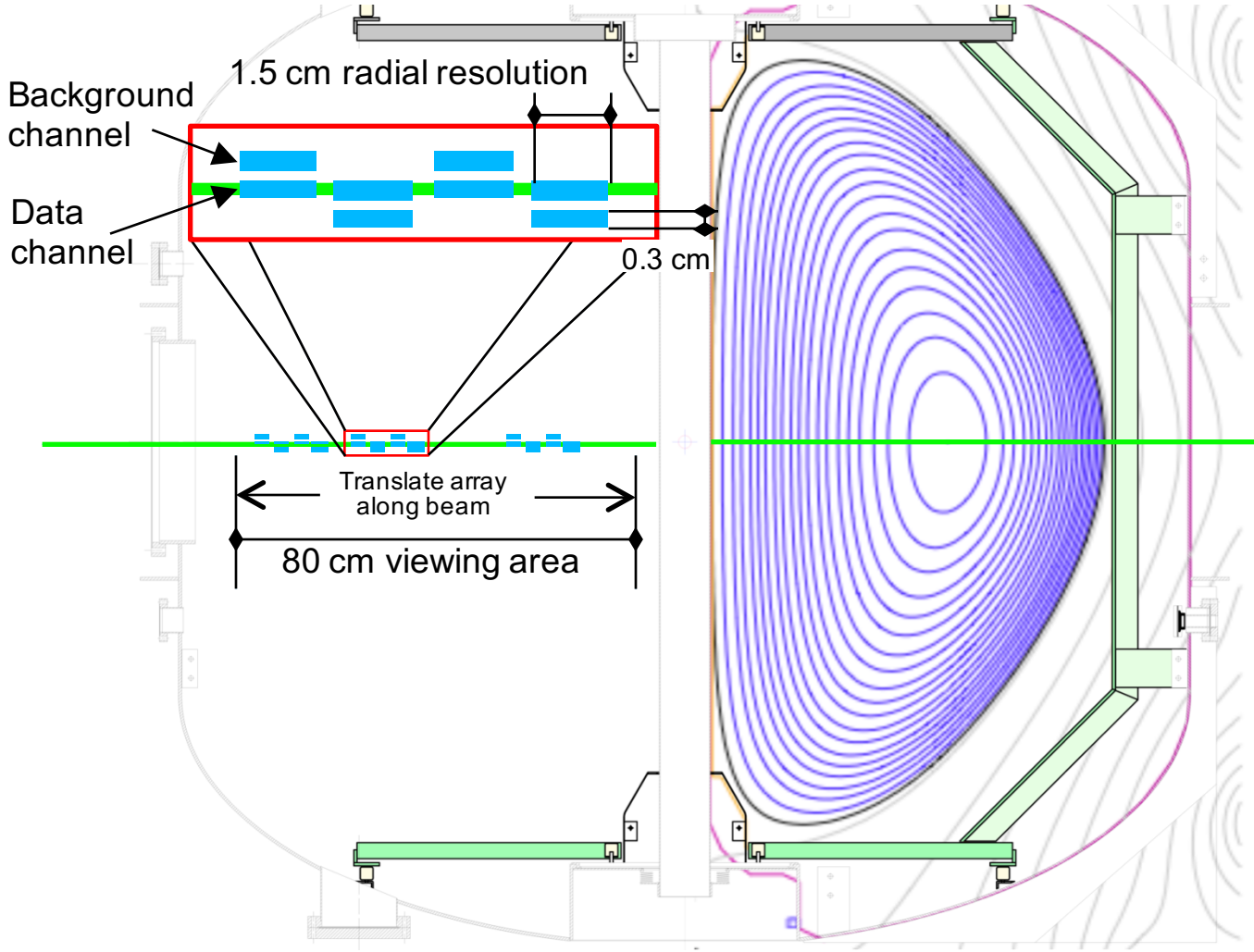
Viewing volumes configured for scattering or background measurements

- Each sample volume: 1.5 cm radial resolution
- Off-laser channels used for co-located background measurements
  - Presently uses data & background pairs



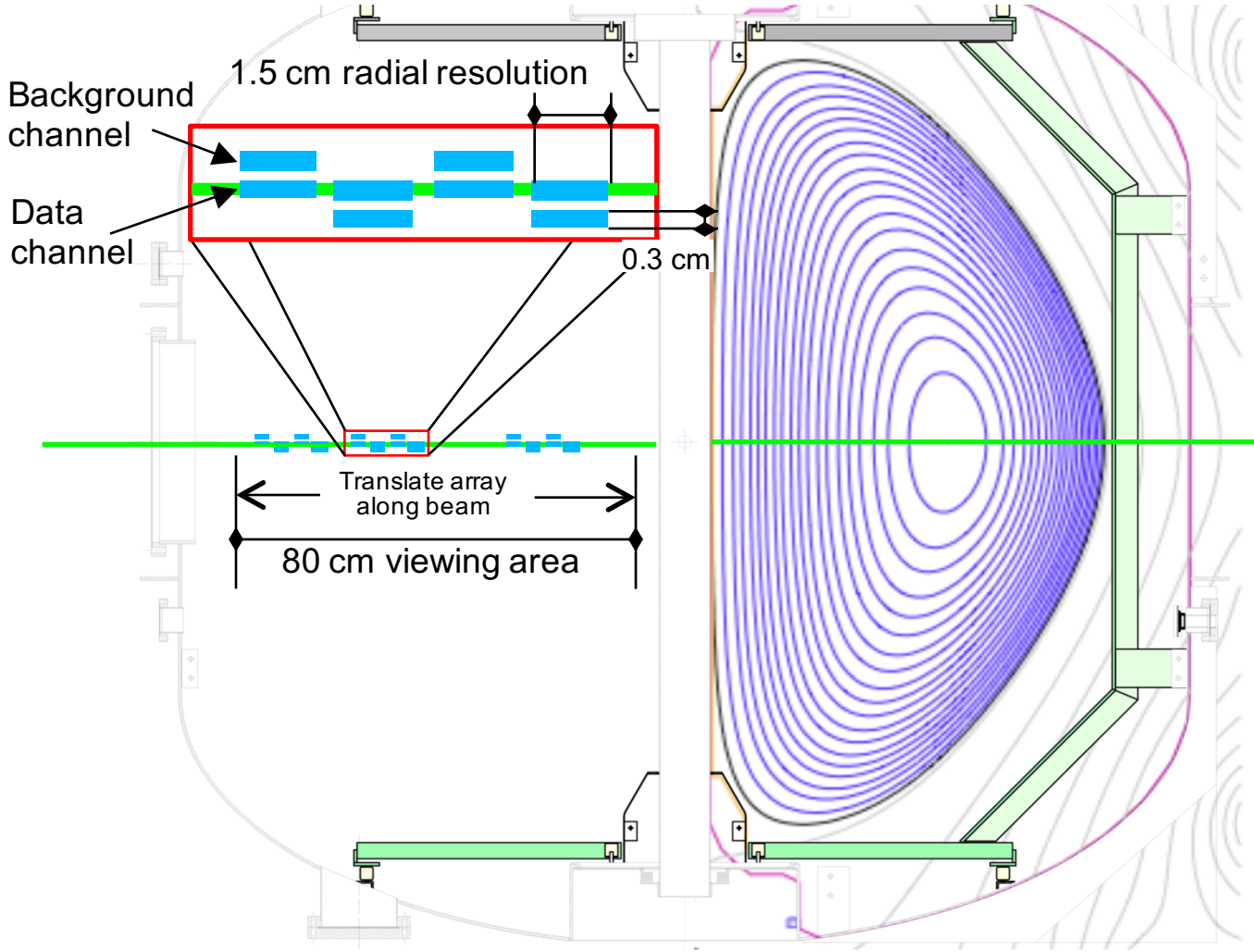
Viewing volumes configured for scattering or background measurements

- Each sample volume: 1.5 cm radial resolution
- Off-laser channels used for co-located background measurements
  - Presently uses data & background pairs
- Channels smoothly translated along major radius at collection optics



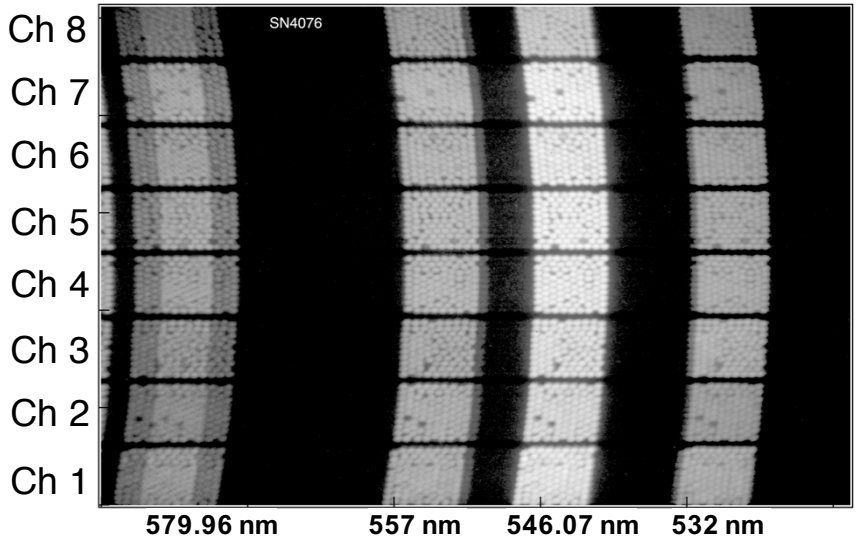
Viewing volumes configured for scattering or background measurements

- Each sample volume: 1.5 cm radial resolution
- Off-laser channels used for co-located background measurements
  - Presently uses data & background pairs
- Channels smoothly translated along major radius at collection optics
- Collection optics are a multi-element, custom lens system
  - 13.4 cm dia. aperture facing plasma
  - F/2 imaging onto fiber bundles



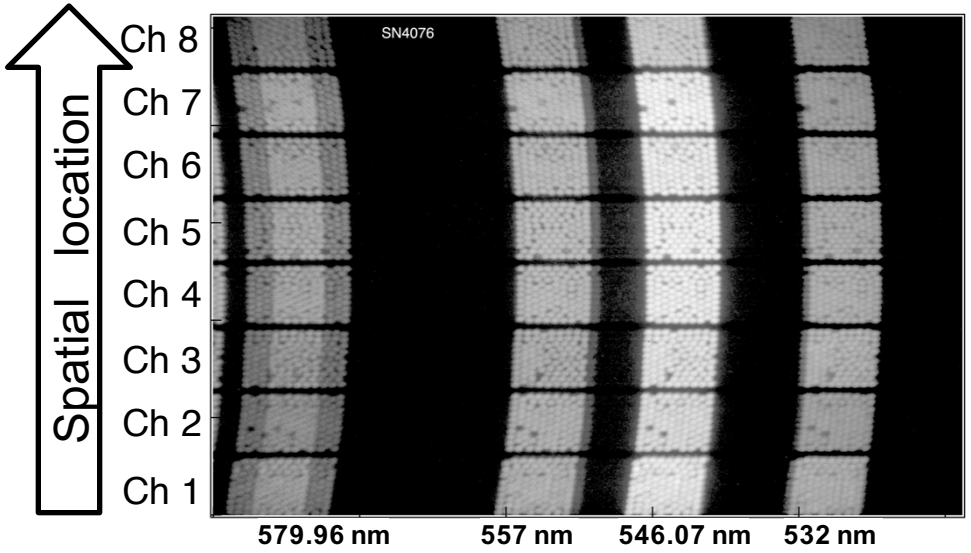
A single ICCD measures 8 spatial locations and all wavelength bins

- Multiple spatial locations imaged onto a single ICCD
  - Spatial location maps vertically on detector
  - Wavelength increases right-to-left on detector
  - 13.3 mm^2 CCDs are 1024 x 1024 pixels



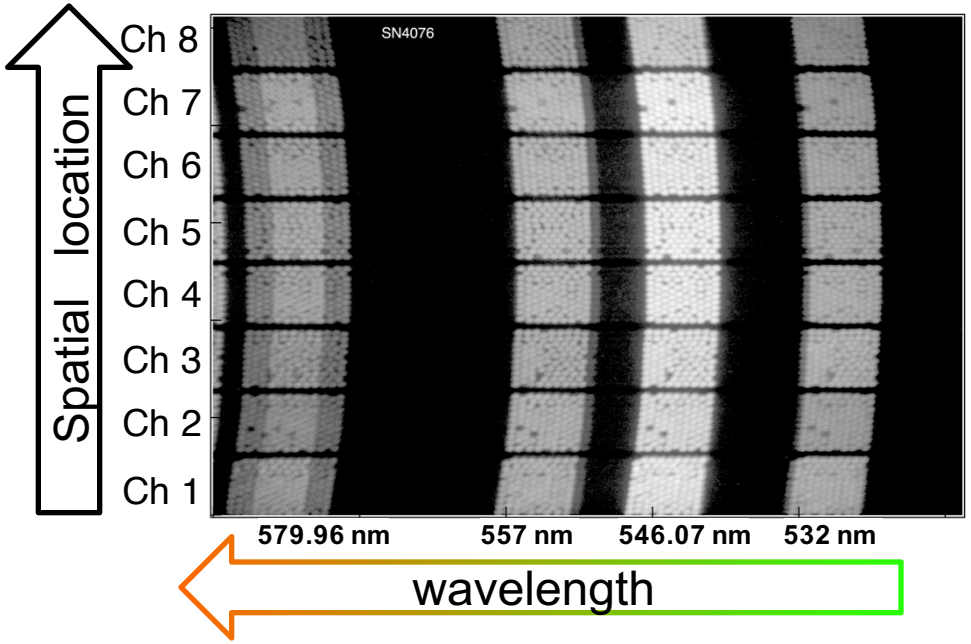
A single ICCD measures 8 spatial locations and all wavelength bins

- Multiple spatial locations imaged onto a single ICCD
  - Spatial location maps vertically on detector
  - Wavelength increases right-to-left on detector
  - 13.3 mm^2 CCDs are 1024 x 1024 pixels



A single ICCD measures 8 spatial locations and all wavelength bins

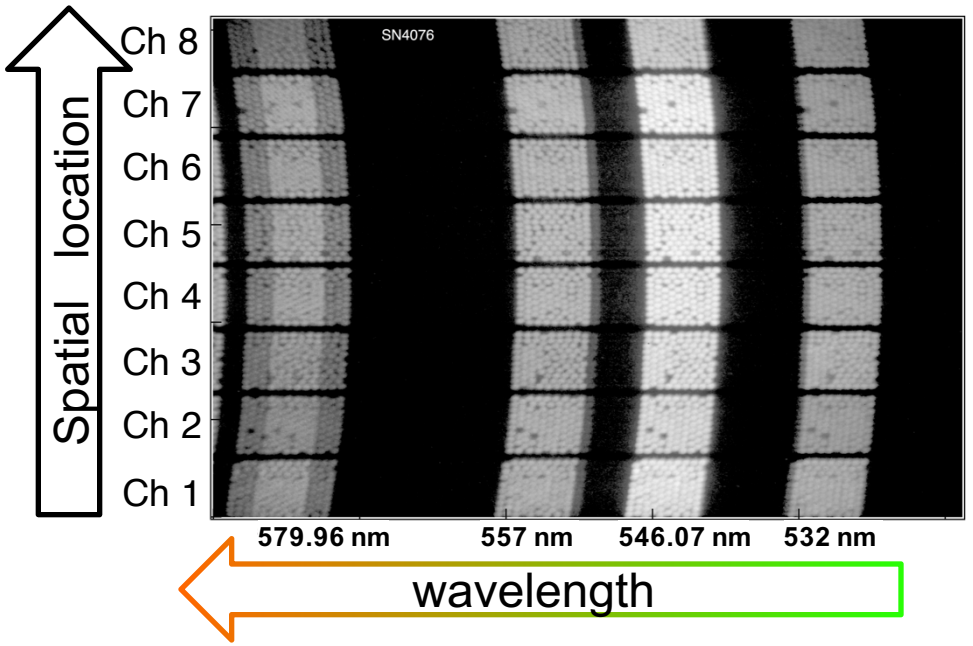
- Multiple spatial locations imaged onto a single ICCD
  - Spatial location maps vertically on detector
  - Wavelength increases right-to-left on detector
  - 13.3 mm^2 CCDs are 1024 x 1024 pixels

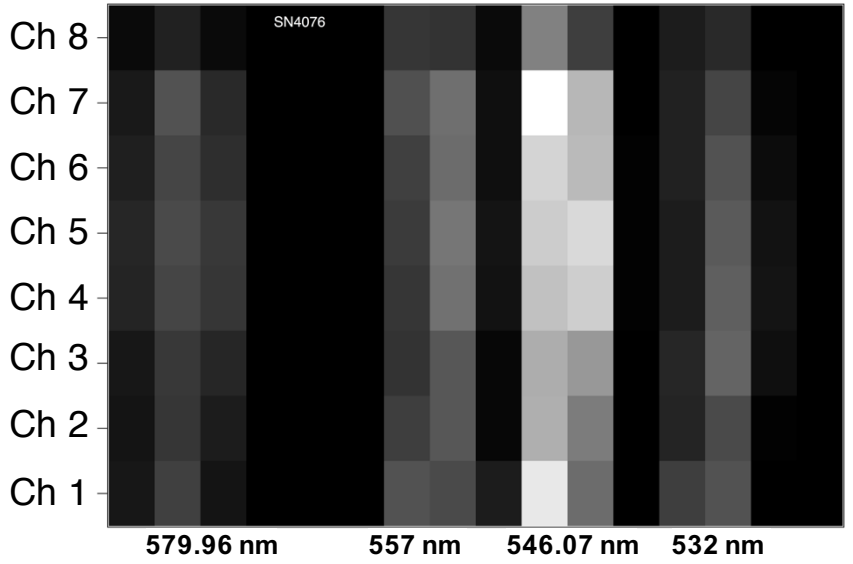


A single ICCD measures 8 spatial locations and all wavelength bins

- Multiple spatial locations imaged onto a single ICCD
  - Spatial location maps vertically on detector
  - Wavelength increases right-to-left on detector
  - 13.3 mm^2 CCDs are 1024 x 1024 pixels

- Binning prior to readout boosts signal-to-noise ratio
  - Bin 64 pix H x ~130 pix V
  - Obtain photon-noise dominated statistics for $n_e > 10^{18}$ m^{-3}



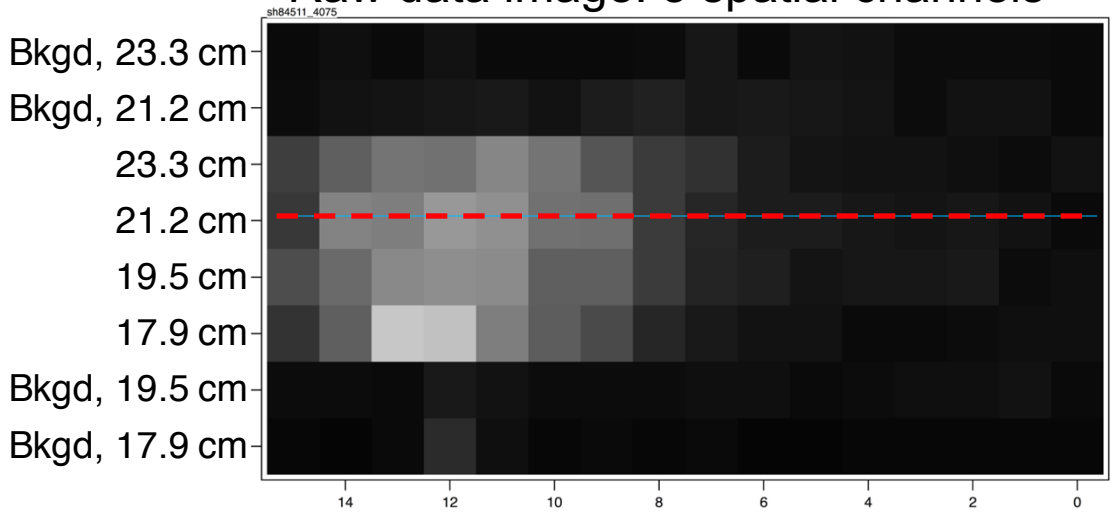


Data flow involves several image processing steps

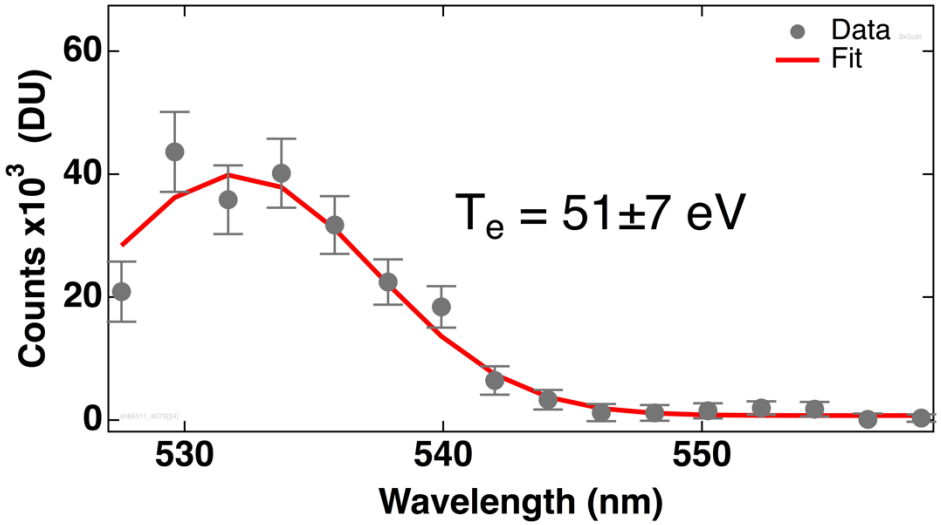
Data Processing Steps:

1. Subtract a dark image (shutter closed)
2. Correct for instrument function
3. Subtract background channel
4. Fit scattered spectrum to obtain T_e

Raw data image: 8 spatial channels



Scattered spectrum from single-shot



Scaleable spectrometer design has built-in data acquisition

Scaleable spectrometer design has built-in data acquisition

- VPH grating provides 1 optic for all wavelength bins

Scaleable spectrometer design has built-in data acquisition

- VPH grating provides 1 optic for all wavelength bins

- ICCD camera provides built-in digitizer
  - Single element samples all wavelength bins
  - Tremendously simplifies data acquisition system

Scaleable spectrometer design has built-in data acquisition

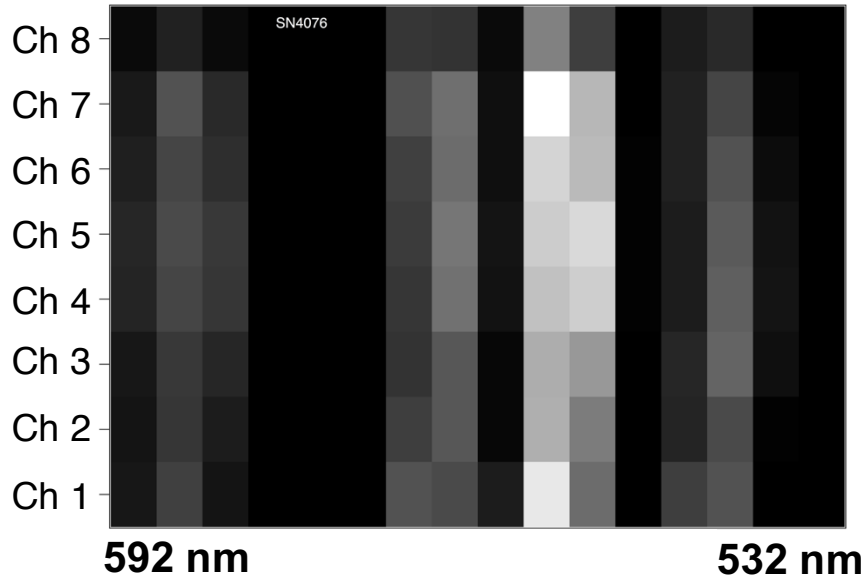
- VPH grating provides 1 optic for all wavelength bins
- ICCD camera provides built-in digitizer
  - Single element samples all wavelength bins
  - Tremendously simplifies data acquisition system
- Spatial channels stacked vertically on detector:
  - 8 spatial channels per spectrometer
  - All wavelength bins for 8 channels acquired by single component (ICCD)





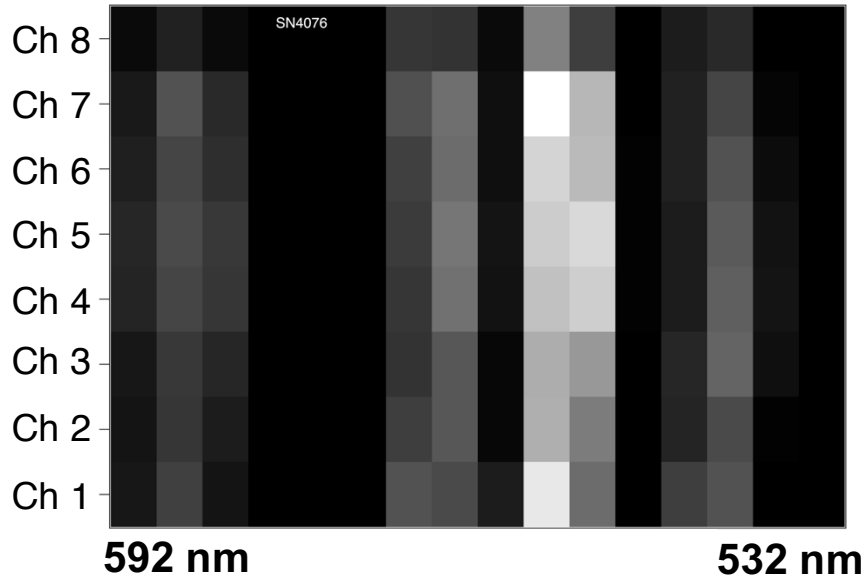
Scaleable spectrometer design has built-in data acquisition

- VPH grating provides 1 optic for all wavelength bins
- ICCD camera provides built-in digitizer
  - Single element samples all wavelength bins
  - Tremendously simplifies data acquisition system
- Spatial channels stacked vertically on detector:
  - 8 spatial channels per spectrometer
  - All wavelength bins for 8 channels acquired by single component (ICCD)



Scaleable spectrometer design has built-in data acquisition

- VPH grating provides 1 optic for all wavelength bins
- ICCD camera provides built-in digitizer
  - Single element samples all wavelength bins
  - Tremendously simplifies data acquisition system
- Spatial channels stacked vertically on detector:
  - 8 spatial channels per spectrometer
  - All wavelength bins for 8 channels acquired by single component (ICCD)
- Result:
  - Readily scaleable system
  - 8 spatial channels,16 spectral bins per single grating/ICCD pair

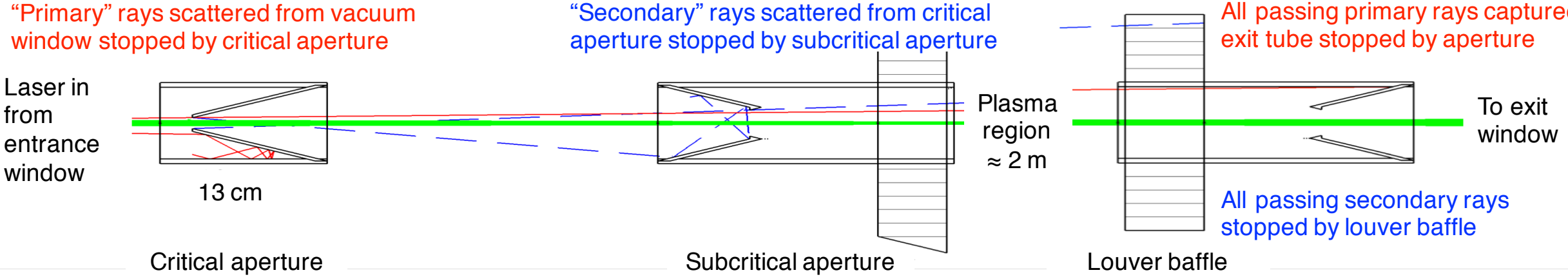


Custom in-vessel baffle system extinguishes stray light

"Primary" rays scattered from vacuum window stopped by critical aperture

"Secondary" rays scattered from critical aperture stopped by subcritical aperture

All passing primary rays captured in exit tube stopped by aperture



Enable 3D View

[1]C.J. Barth et al., Rev. Sci. Instrum. 68 (1997) 3380
J.P. Levesque et al., Rev. Sci. Instrum. 82 (2011) 033501
D.J. Schlossberg J. Instrumentation, **8**, 11, C11019 (2013)

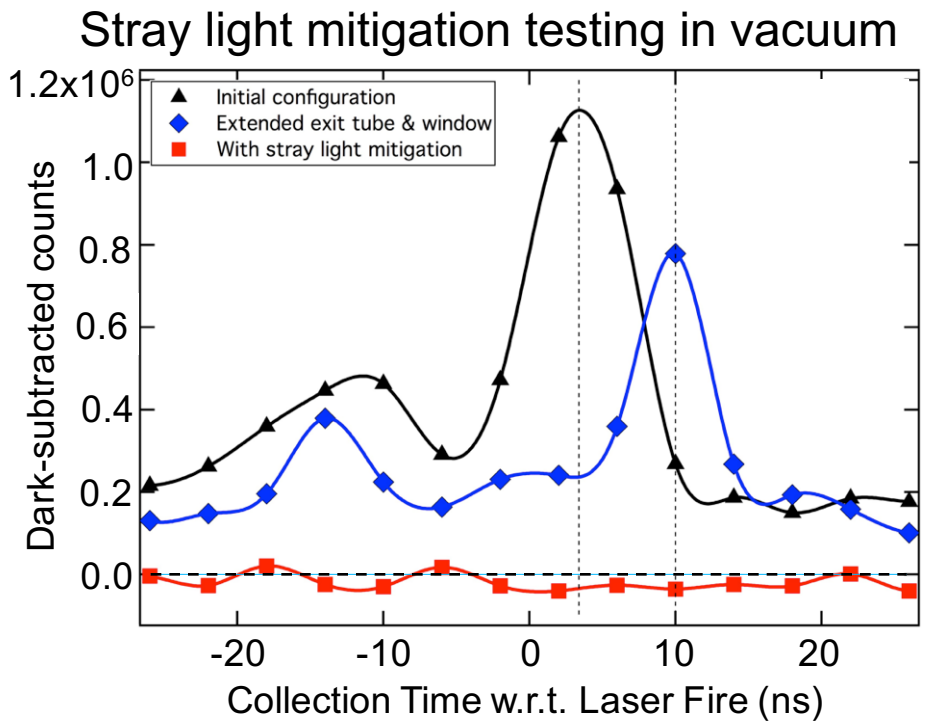
Stray light mitigated by in-vessel baffling and eliminated by time-of-flight rejection

Stray light mitigated by in-vessel baffling and eliminated by time-of-flight rejection

- Collection time window scanned for each step in mitigation process
  - *Sources of stray light identified by change in times of peak stray signal*

Stray light mitigated by in-vessel baffling and eliminated by time-of-flight rejection

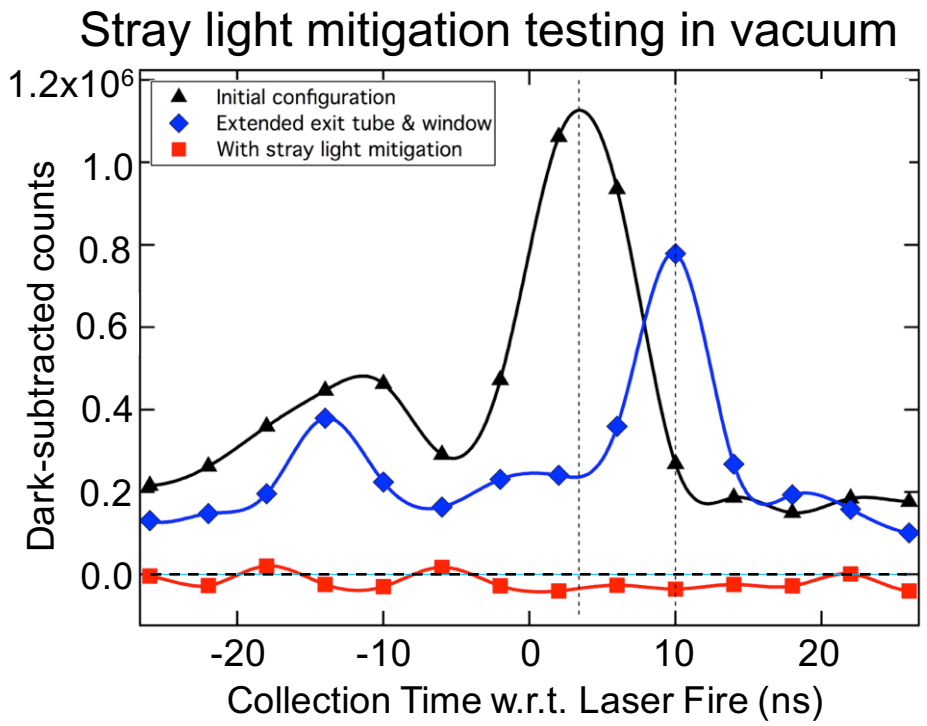
- Collection time window scanned for each step in mitigation process
  - *Sources of stray light identified by change in times of peak stray signal*



D.J. Schlossberg, HTPD 2016

Stray light mitigated by in-vessel baffling and eliminated by time-of-flight rejection

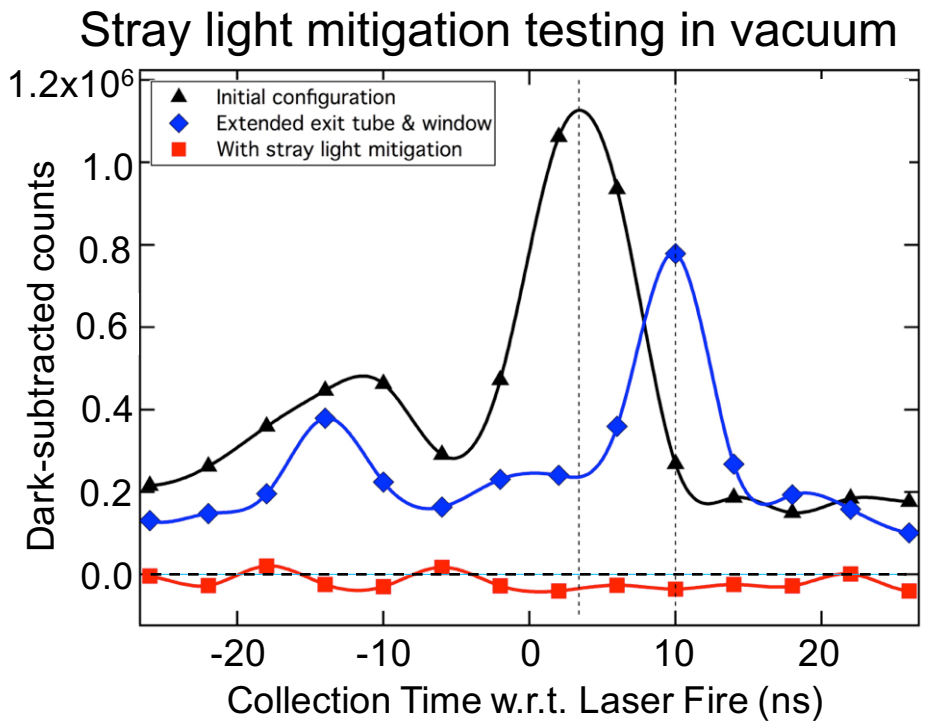
- Collection time window scanned for each step in mitigation process
  - *Sources of stray light identified by change in times of peak stray signal*
- Stray light levels sufficiently reduced using apertures



D.J. Schlossberg, HTPD 2016

Stray light mitigated by in-vessel baffling and eliminated by time-of-flight rejection

- Collection time window scanned for each step in mitigation process
  - *Sources of stray light identified by change in times of peak stray signal*
- Stray light levels sufficiently reduced using apertures
- Time-of-flight rejection eliminates remaining stray light component

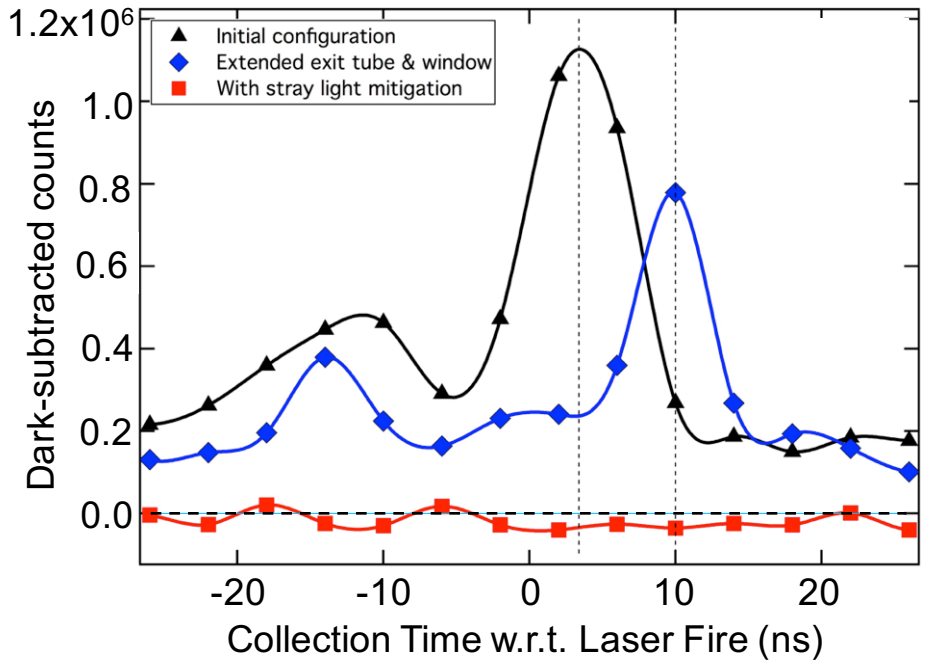


D.J. Schlossberg, HTPD 2016

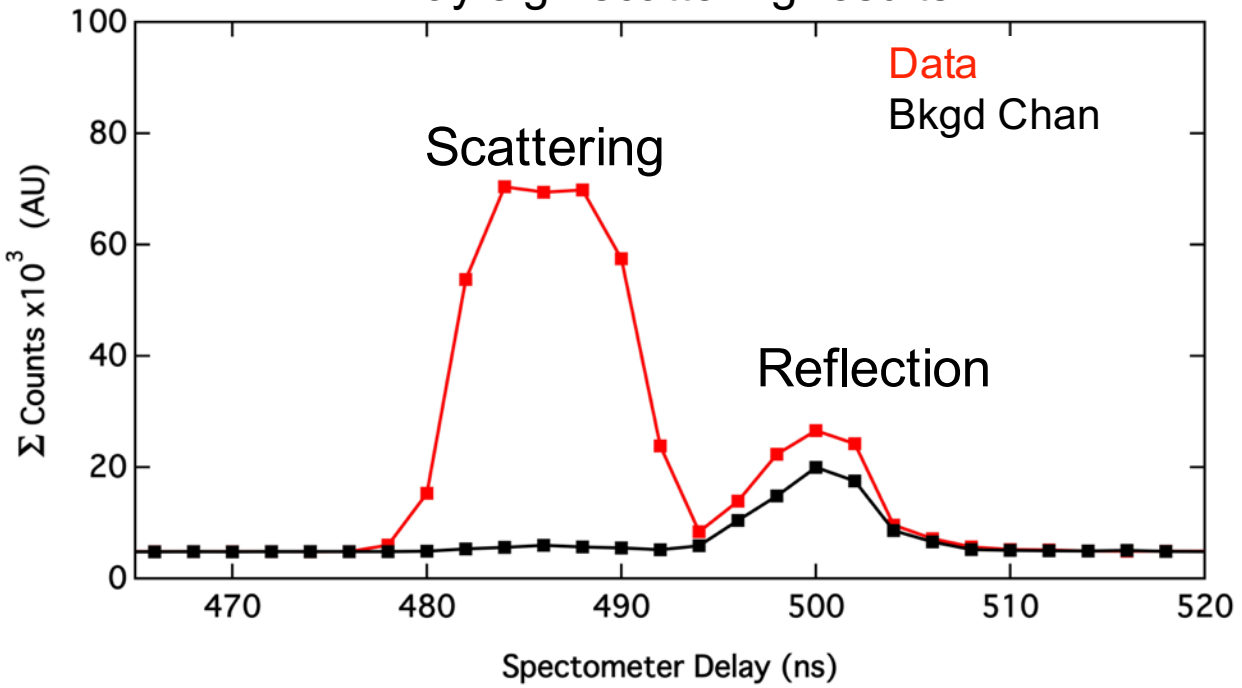
Stray light mitigated by in-vessel baffling and eliminated by time-of-flight rejection

- Collection time window scanned for each step in mitigation process
  - *Sources of stray light identified by change in times of peak stray signal*
- Stray light levels sufficiently reduced using apertures
- Time-of-flight rejection eliminates remaining stray light component

Stray light mitigation testing in vacuum

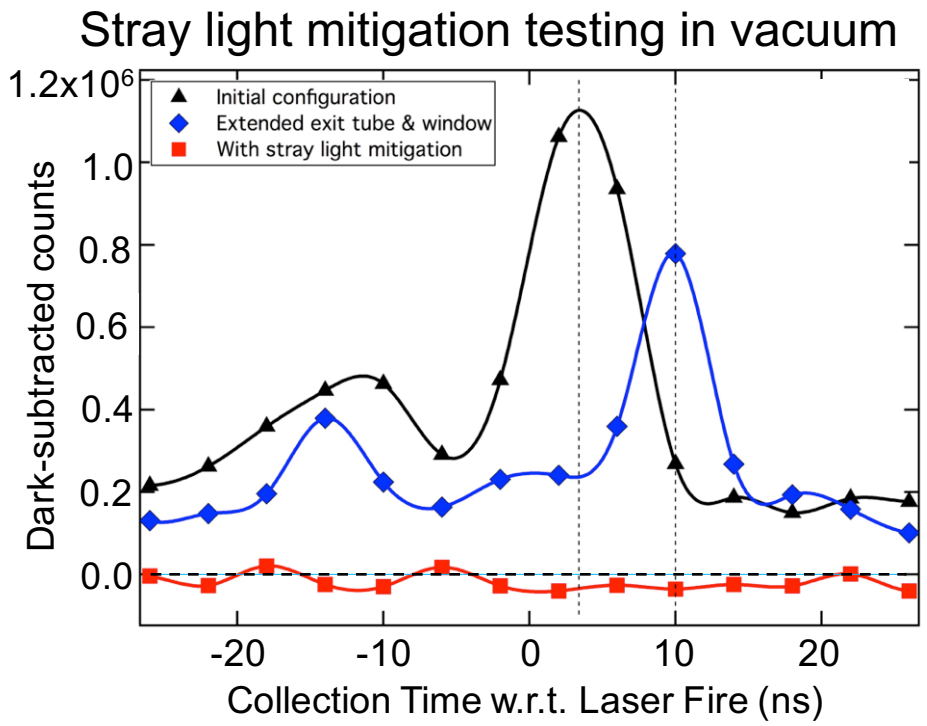


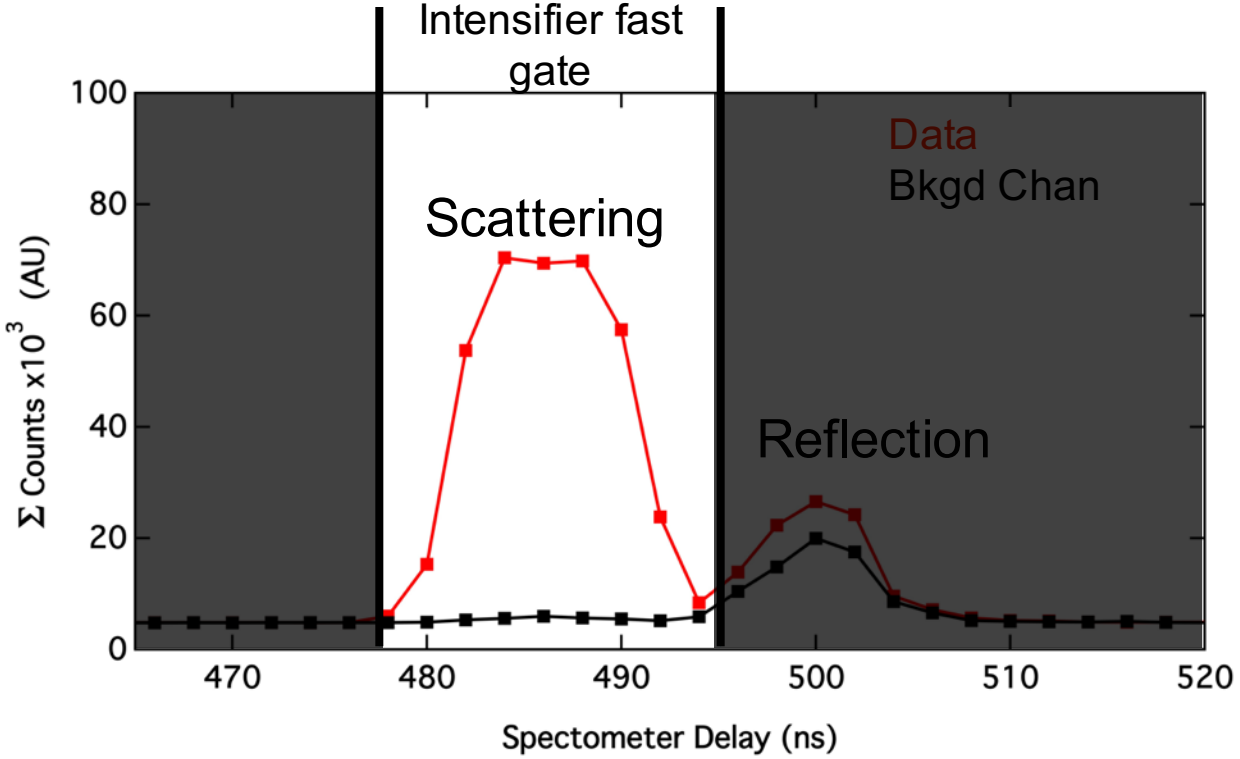
Rayleigh scattering results



Stray light mitigated by in-vessel baffling and eliminated by time-of-flight rejection

- Collection time window scanned for each step in mitigation process
  - *Sources of stray light identified by change in times of peak stray signal*
- Stray light levels sufficiently reduced using apertures
- Time-of-flight rejection eliminates remaining stray light component



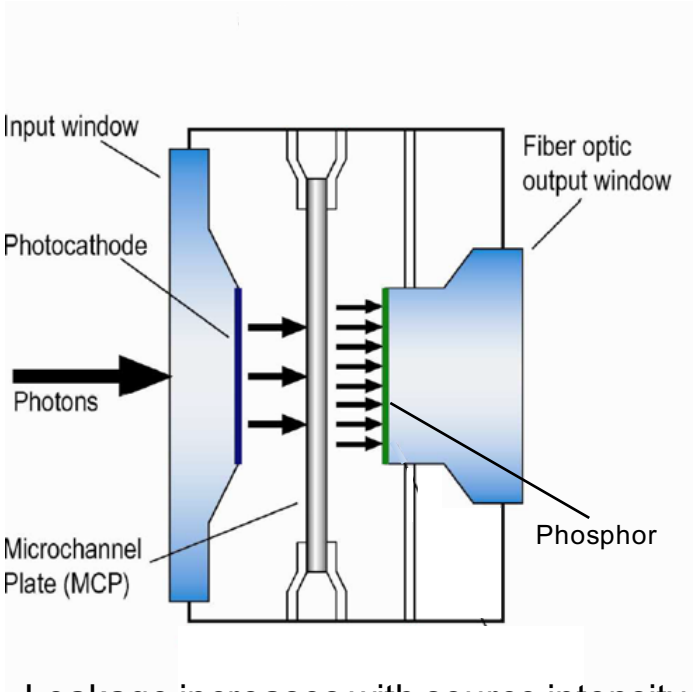


D.J. Schlossberg, HTPD 2016

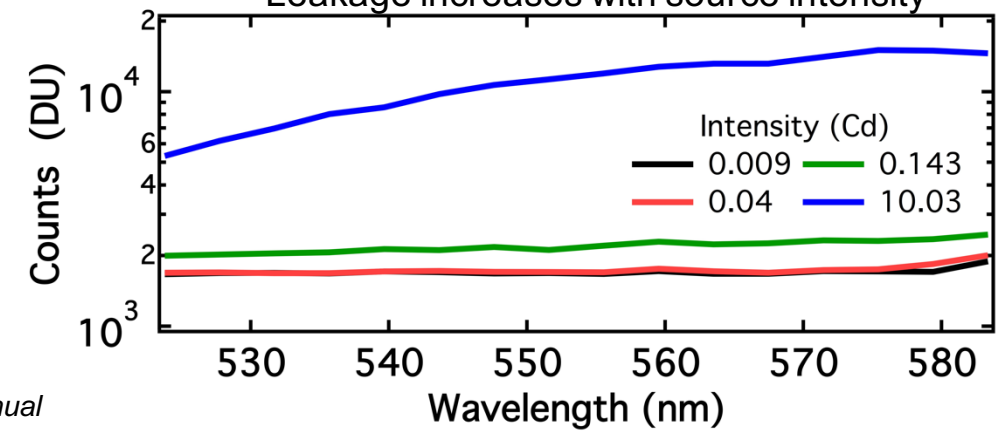
Background light observed when photocathode voltage is off

- Image intensifiers comprise:
  - Photocathode — ph → e-
  - Micro-channel plate (MCP) — e- → many e-
  - Phosphor — e- → ph
- ICCD fast-gating switches the photocathode voltage
- During operations anomalous background levels observed
- During calibration, image intensifier leakage confirmed
  - Continuous, calibrated source used
  - Intensities similar to plasma operations

ICCD image intensifier schematic



Leakage increases with source intensity

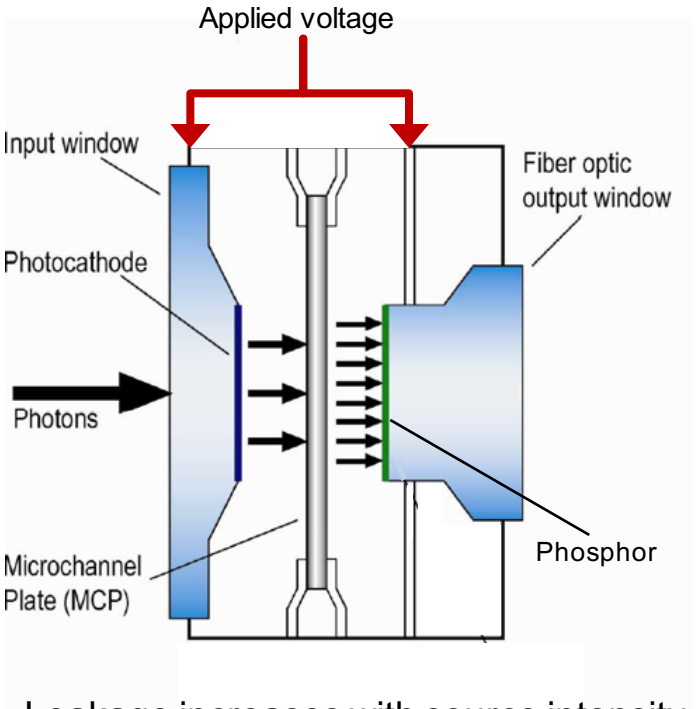


Intensifier schematic from Andor iStar ICCD User Manual

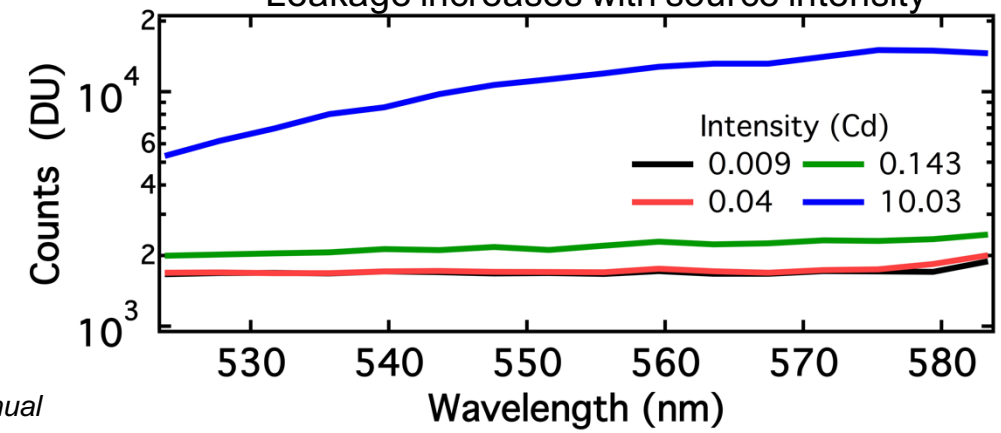
Background light observed when photocathode voltage is off

- Image intensifiers comprise:
  - Photocathode — ph → e-
  - Micro-channel plate (MCP) — e- → many e-
  - Phosphor — e- → ph
- ICCD fast-gating switches the photocathode voltage
- During operations anomalous background levels observed
- During calibration, image intensifier leakage confirmed
  - Continuous, calibrated source used
  - Intensities similar to plasma operations

ICCD image intensifier schematic



Leakage increases with source intensity



Intensifier schematic from Andor iStar ICCD User Manual

High speed, high transmission shutter developed to block leakage

High speed, high transmission shutter developed to block leakage

- CCD readout time long (~ms) compared to collection gate (~ns)
  - Initially used irising shutter in front of camera
  - 13 ms closed-open-closed time





High speed, high transmission shutter developed to block leakage

- CCD readout time long (~ms) compared to collection gate (~ns)
  - Initially used irising shutter in front of camera
  - 13 ms closed-open-closed time

- **Need:** fast (< 1 ms), high transmission shutter
  - Hard to find! (any ideas?...)





High speed, high transmission shutter developed to block leakage

- CCD readout time long (~ms) compared to collection gate (~ns)
  - Initially used irising shutter in front of camera
  - 13 ms closed-open-closed time

- **Need:** fast (< 1 ms), high transmission shutter
  - Hard to find! (any ideas?...)

- **Solution:** Adapt a hard drive read-arm for optical shuttering[1]

- **Implementation:**
  - Place in front of spectrometer's entrance slit



[1]R.E. Scholten, Rev. Sci. Instrum. **78**, 026101 (2007)



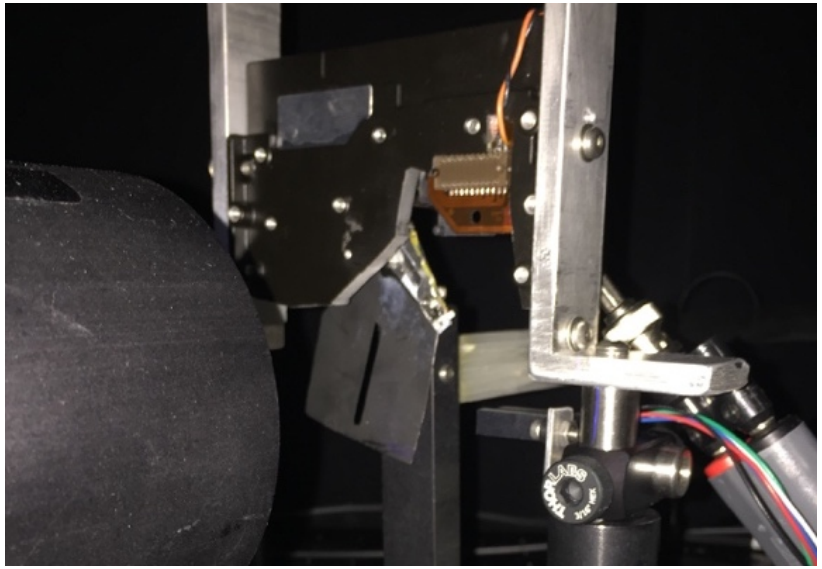
High speed, high transmission shutter developed to block leakage

- CCD readout time long (~ms) compared to collection gate (~ns)
  - Initially used irising shutter in front of camera
  - 13 ms closed-open-closed time

- **Need:** fast (< 1 ms), high transmission shutter
  - Hard to find! (any ideas?...)

- **Solution:** Adapt a hard drive read-arm for optical shuttering[1]

- **Implementation:**
  - Place in front of spectrometer's entrance slit



[1]R.E. Scholten, Rev. Sci. Instrum. **78**, 026101 (2007)

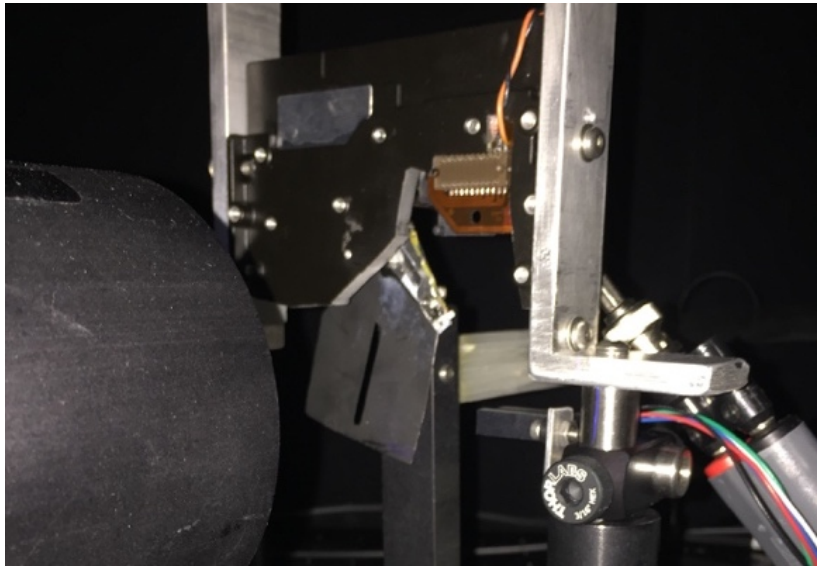
High speed, high transmission shutter developed to block leakage

- CCD readout time long (~ms) compared to collection gate (~ns)
  - Initially used irising shutter in front of camera
  - 13 ms closed-open-closed time

- **Need:** fast (< 1 ms), high transmission shutter
  - Hard to find! (any ideas?...)

- **Solution:** Adapt a hard drive read-arm for optical shuttering[1]

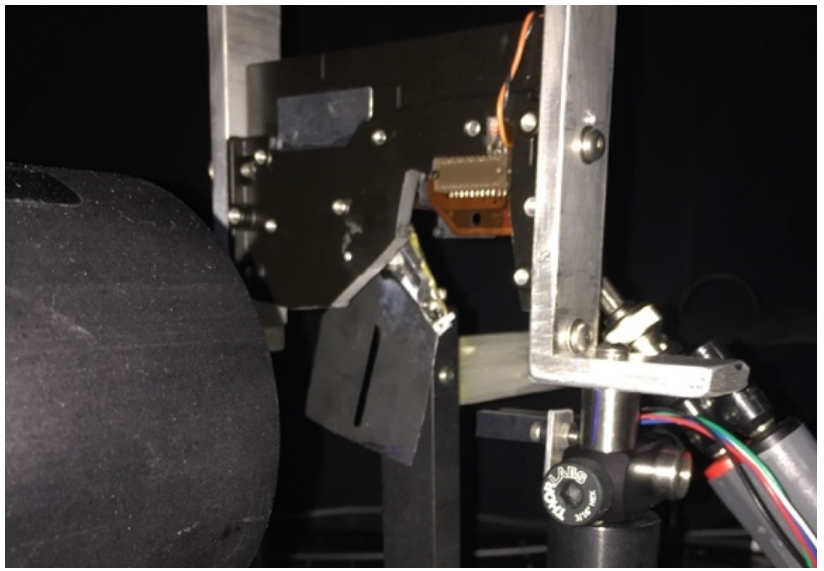
- **Implementation:**
  - Place in front of spectrometer's entrance slit
  - Open time and jitter characterized
  - Integrate into tightly-timed Thomson fire sequence



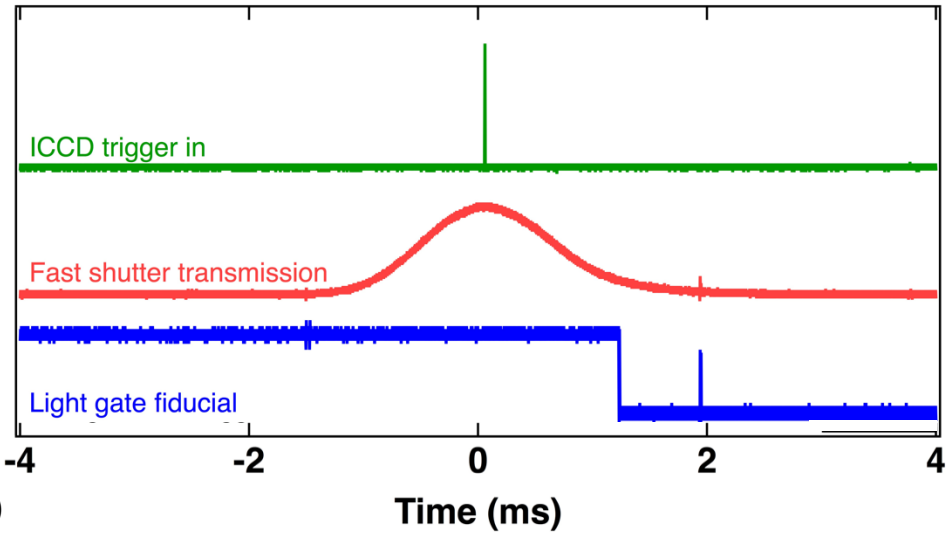
[1]R.E. Scholten, Rev. Sci. Instrum. **78**, 026101 (2007)

High speed, high transmission shutter developed to block leakage

- CCD readout time long (~ms) compared to collection gate (~ns)
  - Initially used irising shutter in front of camera
  - 13 ms closed-open-closed time
- **Need:** fast (< 1 ms), high transmission shutter
  - Hard to find! (any ideas?...)
- **Solution:** Adapt a hard drive read-arm for optical shuttering[1]
- **Implementation:**
  - Place in front of spectrometer's entrance slit
  - Open time and jitter characterized
  - Integrate into tightly-timed Thomson fire sequence



Fast shutter timing data, SN4076

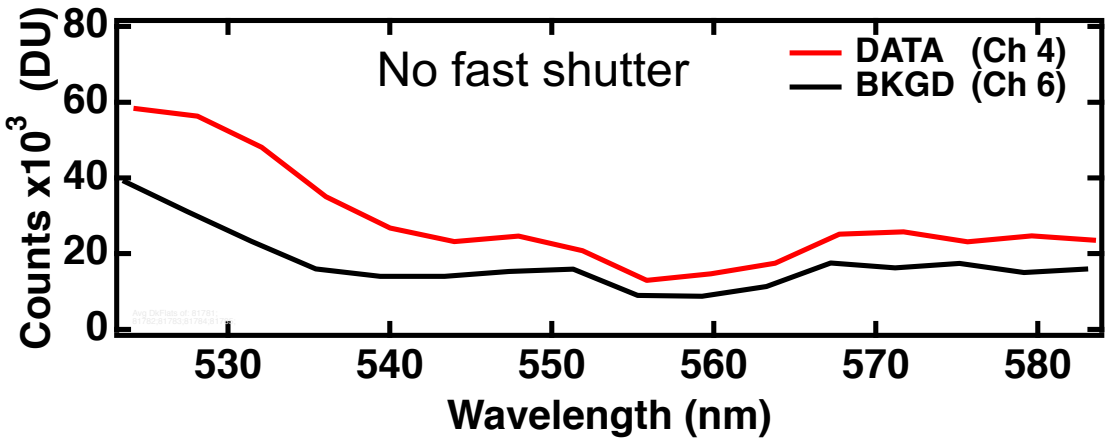


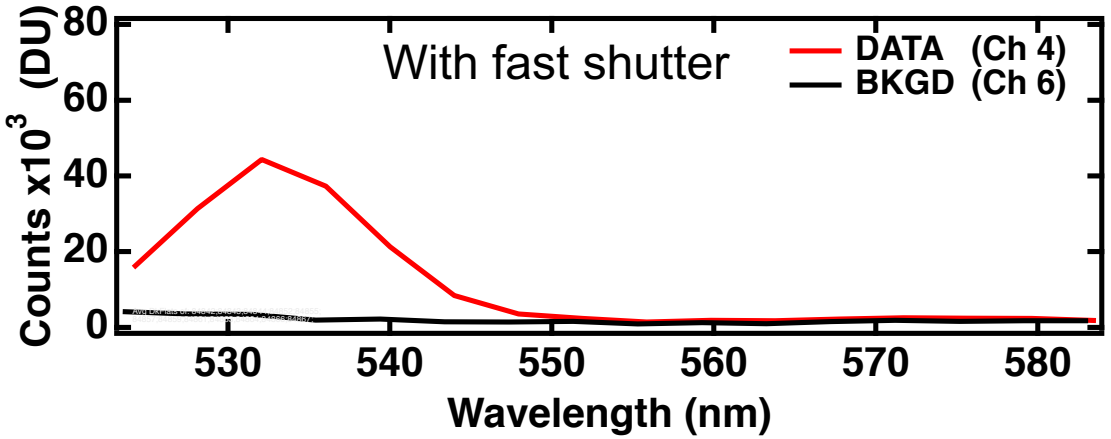
[1]R.E. Scholten, Rev. Sci. Instrum. **78**, 026101 (2007)

Fast shuttering dramatically reduces background light collected

- Observe typical Pegasus plasmas
  - Repeat measurement to gather statistics
- Process data and average results
- Repeat using fast shutter
  - Identical diagnostic settings (gain, etc)
  - *Different location for helicity injectors*

Sample Thomson spectra with and without shutters





Initial results: L-mode plasmas used to prove diagnostic operation

- Observe typical Pegasus L-mode plasmas
  - $I_p \sim 170$ kA, $\langle n_e \rangle \sim 1.5 \times 10^{19}$ m^{-3}





Initial results: L-mode plasmas used to prove diagnostic operation

- Observe typical Pegasus L-mode plasmas
  - $I_p \sim 170$ kA, $\langle n_e \rangle \sim 1.5 \times 10^{19}$ m^{-3}

- Data averaged over spatial points and multiple shots





Initial results: L-mode plasmas used to prove diagnostic operation

- Observe typical Pegasus L-mode plasmas
  - $I_p \sim 170$ kA, $\langle n_e \rangle \sim 1.5 \times 10^{19}$ m^{-3}
- Data averaged over spatial points and multiple shots
- First data[1]: high quality spectrum for 10 shot, 4 spatial location average
  - Initial measurements made before optimization

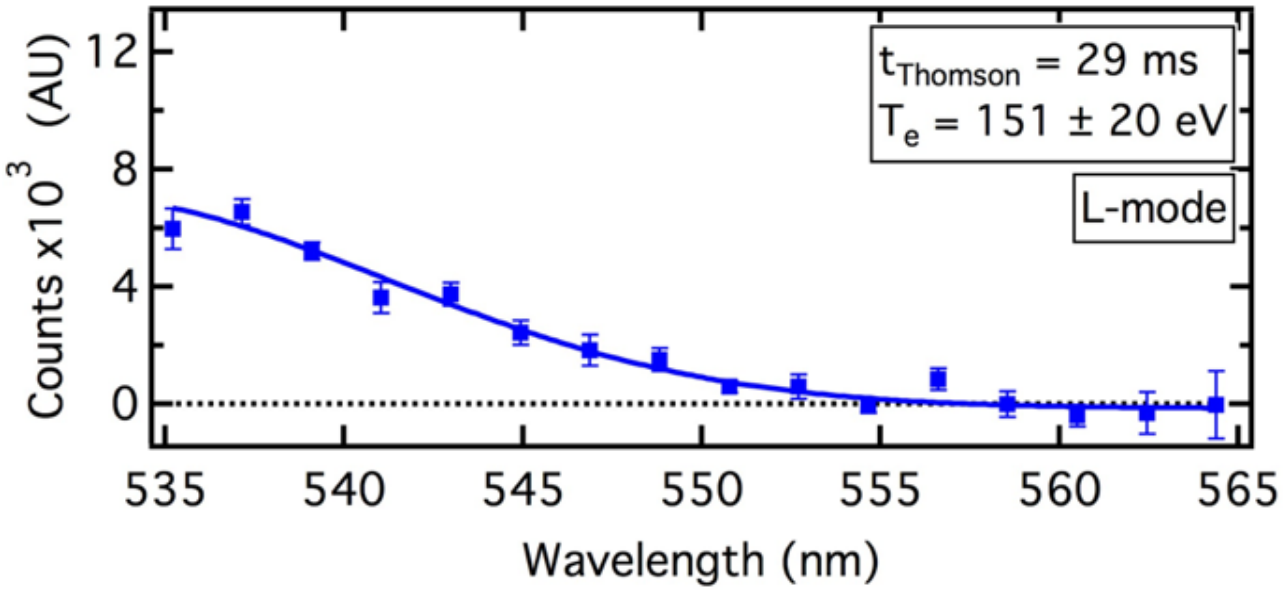


[1] D.J. Schlossberg, J. Instrumentation, **8**, 11, C11019 (2013).



Initial results: L-mode plasmas used to prove diagnostic operation

- Observe typical Pegasus L-mode plasmas
  - $I_p \sim 170$ kA, $\langle n_e \rangle \sim 1.5 \times 10^{19}$ m^{-3}
- Data averaged over spatial points and multiple shots
- First data[1]: high quality spectrum for 10 shot, 4 spatial location average
  - Initial measurements made before optimization

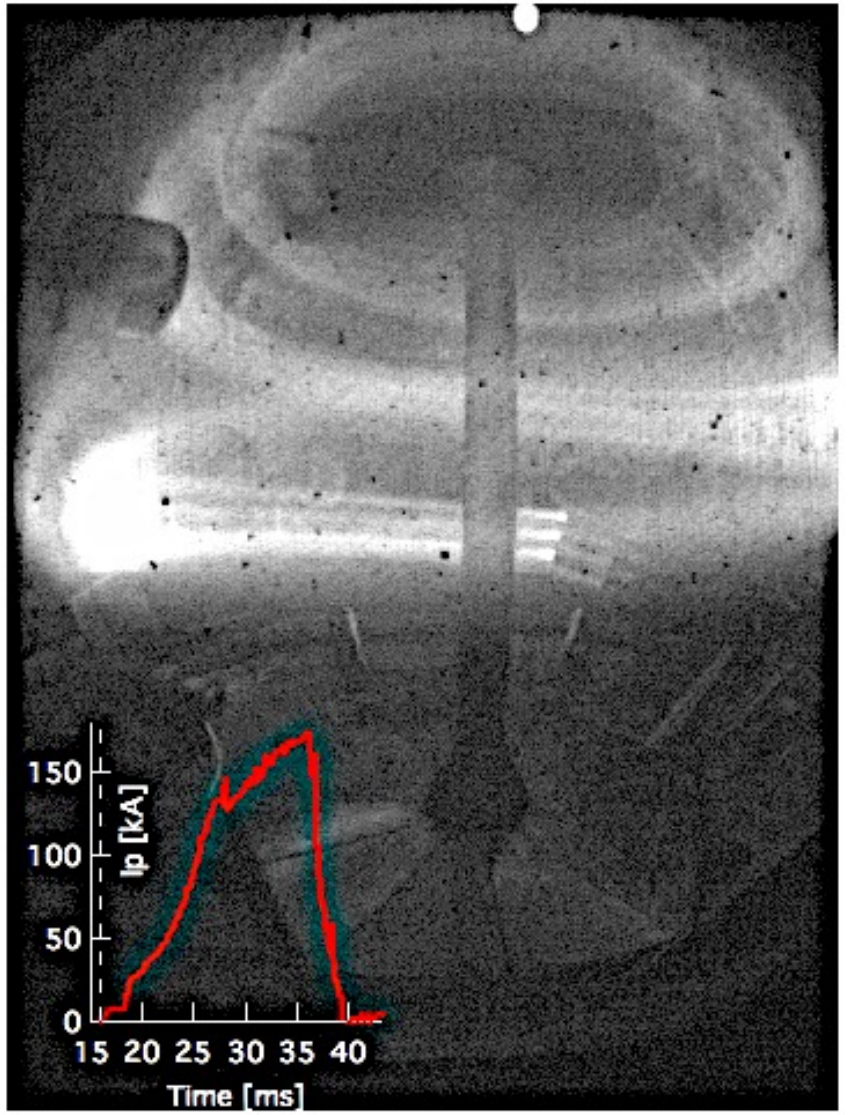


[1] *D.J. Schlossberg, J. Instrumentation,* ***8****, 11, C11019 (2013).*

Pegasus LHI plasmas present unique measurement challenges

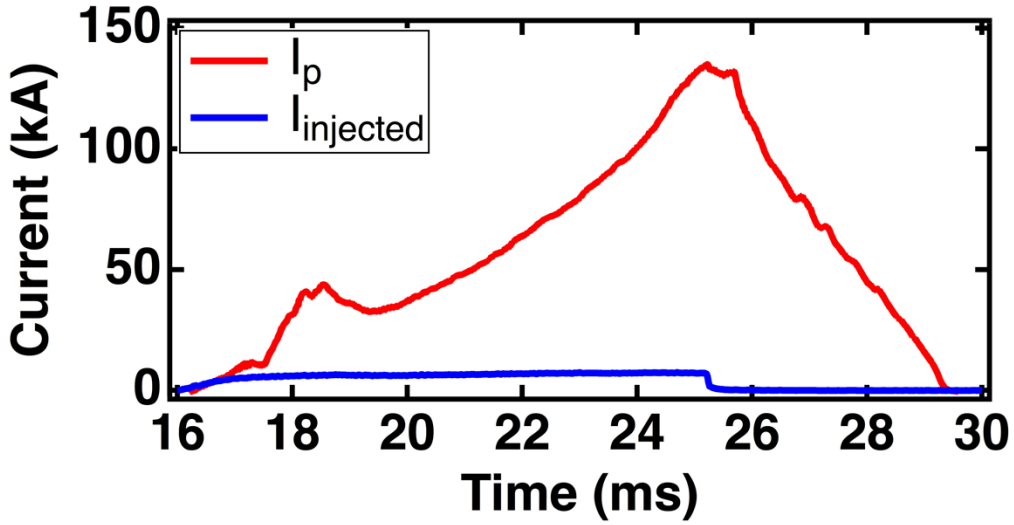
Local Helicity Injection (LHI) drives ~200 kA start-up plasmas non-solenoidally:

- Large MHD, strong magnetic reconnection events
- High background levels with injectors
- Magnetic field stochasticization
  - Effects on T_e profiles
- Strong heating and current source in plasma edge

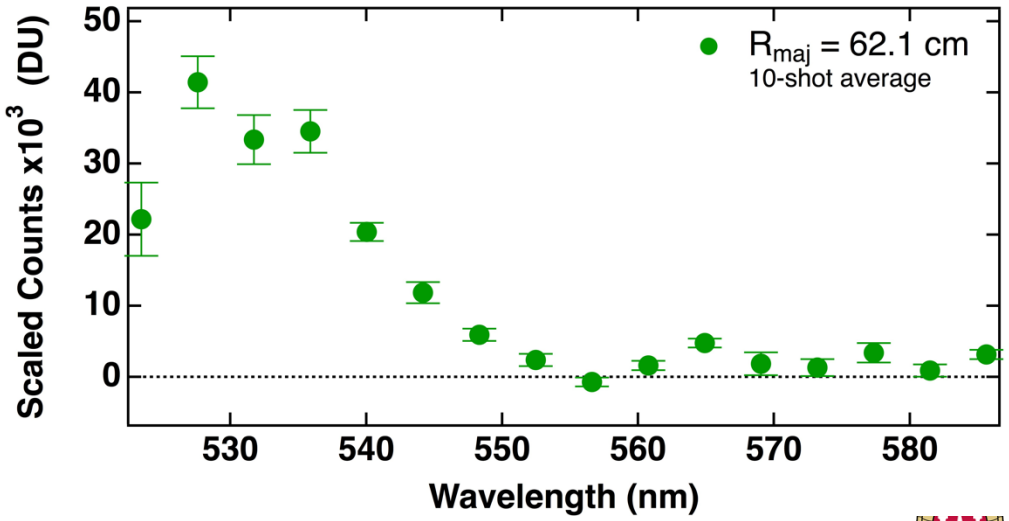


Initial results from LHI plasmas highlight dynamic T_e evolution

- Plasma centroid evolves inward
  - 3 injectors located on outboard side below midplane
- LHI plasmas typically lower density than Ohmic
  - $\langle n_e \rangle \sim 5 \times 10^{18}$ m^{-3}
  - Ensemble average Thomson data to increase SNR *(prior to fast shutter implementation)*



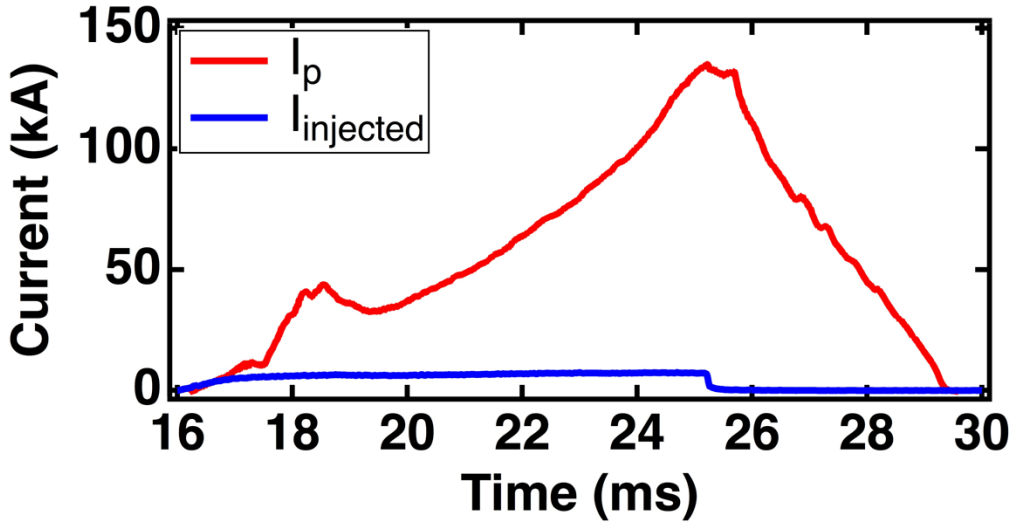
Processed data shows clear Gaussian



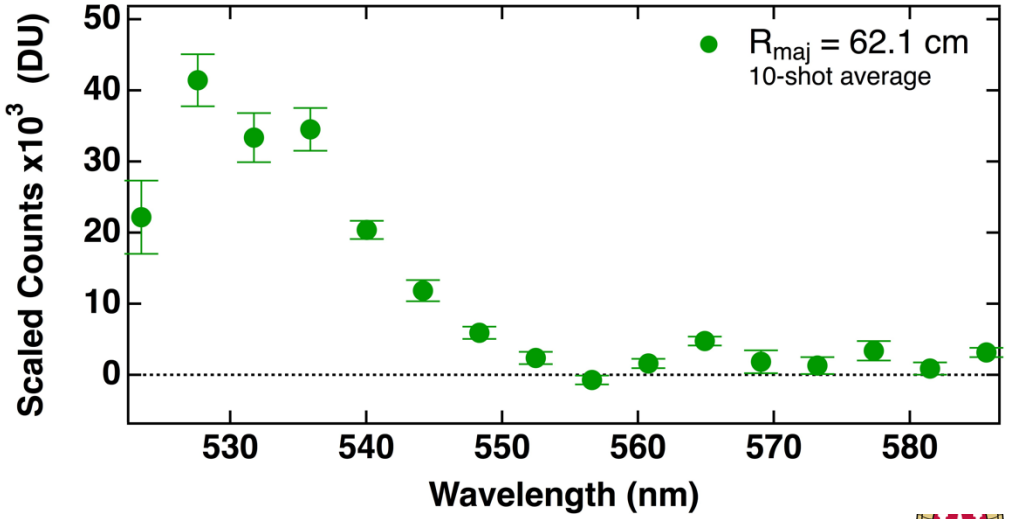
* D.J. Battaglia, et al., Phys. Rev. Lett. **102**, 225003 (2009)

Initial results from LHI plasmas highlight dynamic T_e evolution

- Plasma centroid evolves inward
  - 3 injectors located on outboard side below midplane
- LHI plasmas typically lower density than Ohmic
  - $\langle n_e \rangle \sim 5 \times 10^{18}$ m^{-3}
  - Ensemble average Thomson data to increase SNR *(prior to fast shutter implementation)*
- T_e profiles reveal dynamic evolution:



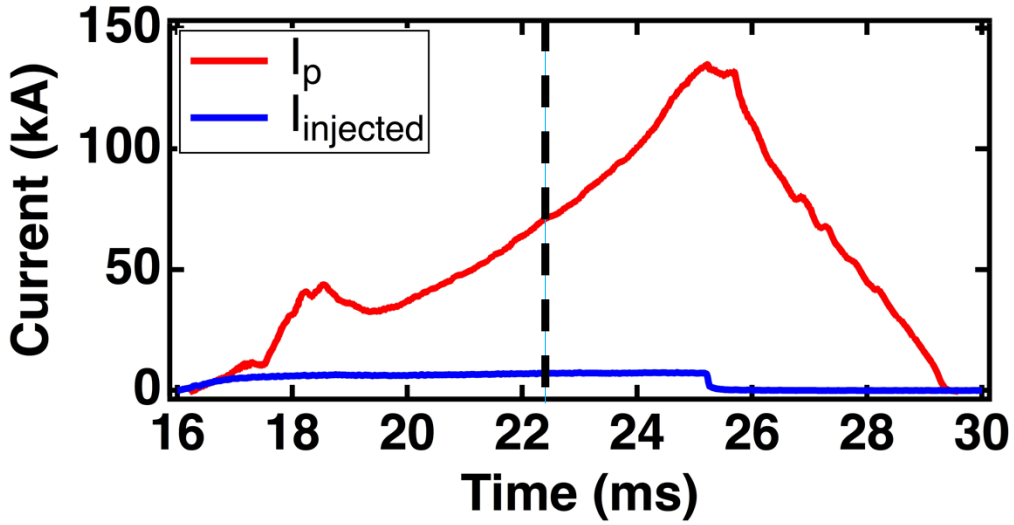
Processed data shows clear Gaussian

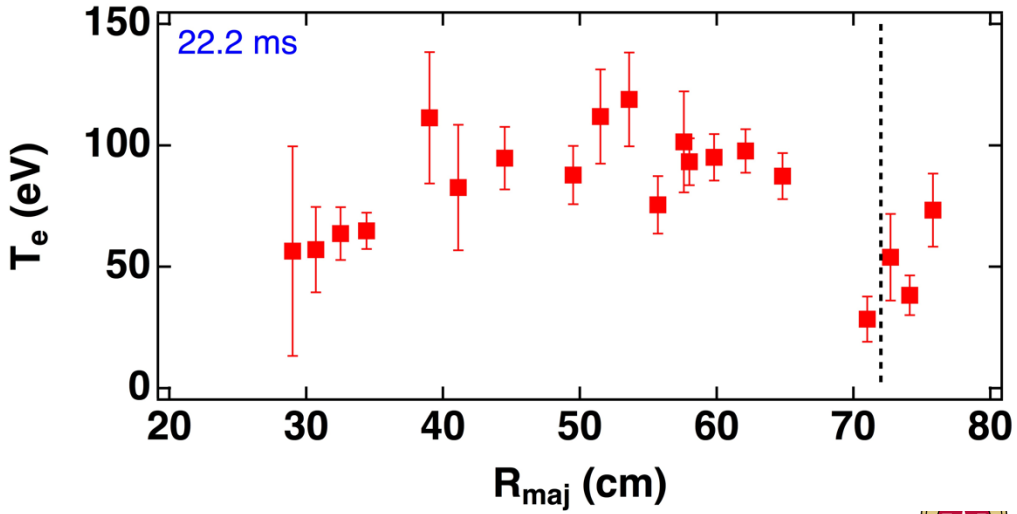


* D.J. Battaglia, et al., Phys. Rev. Lett. **102**, 225003 (2009)

Initial results from LHI plasmas highlight dynamic T_e evolution

- Plasma centroid evolves inward
  - 3 injectors located on outboard side below midplane
- LHI plasmas typically lower density than Ohmic
  - $\langle n_e \rangle \sim 5 \times 10^{18}$ m^{-3}
  - Ensemble average Thomson data to increase SNR *(prior to fast shutter implementation)*
- T_e profiles reveal dynamic evolution:

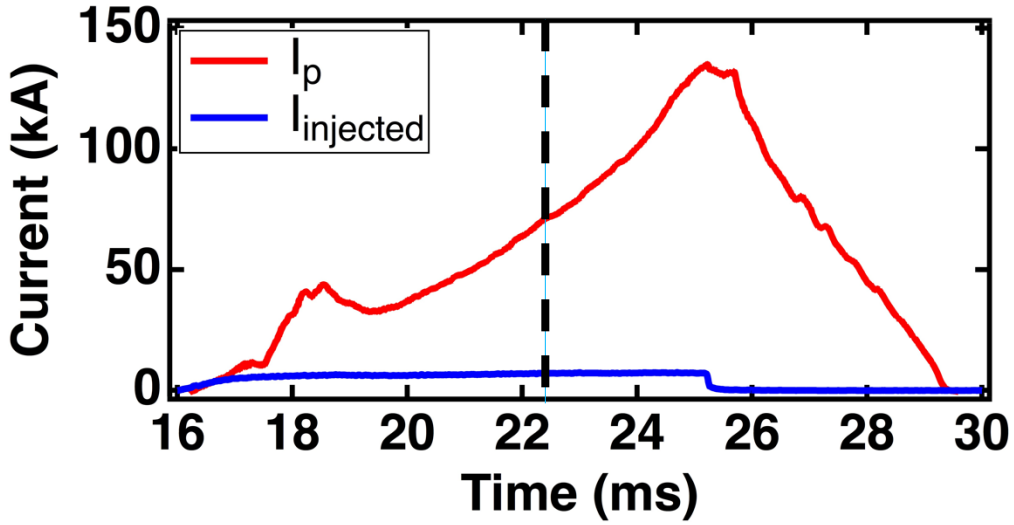


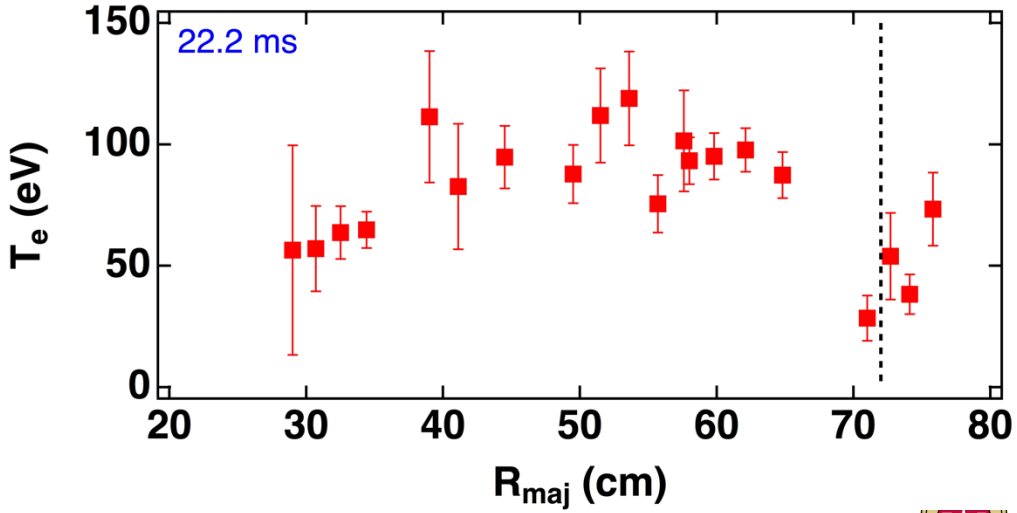


* D.J. Battaglia, et al., Phys. Rev. Lett. **102**, 225003 (2009)

Initial results from LHI plasmas highlight dynamic T_e evolution

- Plasma centroid evolves inward
  - 3 injectors located on outboard side below midplane
- LHI plasmas typically lower density than Ohmic
  - $\langle n_e \rangle \sim 5 \times 10^{18}$ m^{-3}
  - Ensemble average Thomson data to increase SNR *(prior to fast shutter implementation)*
- T_e profiles reveal dynamic evolution:
  - t = 22.2 ms: peaked core T_e, cool injector region
    plasma strongly coupled to outboard drive

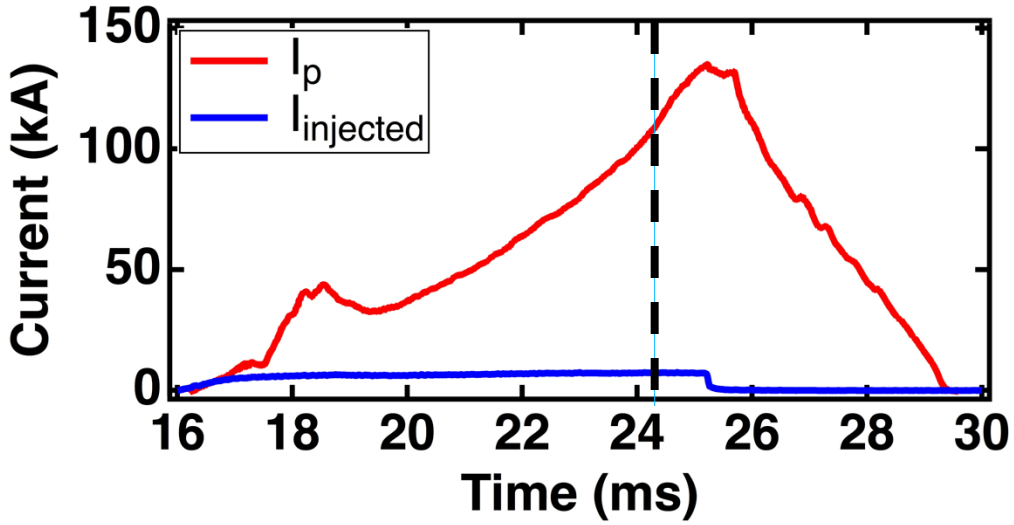


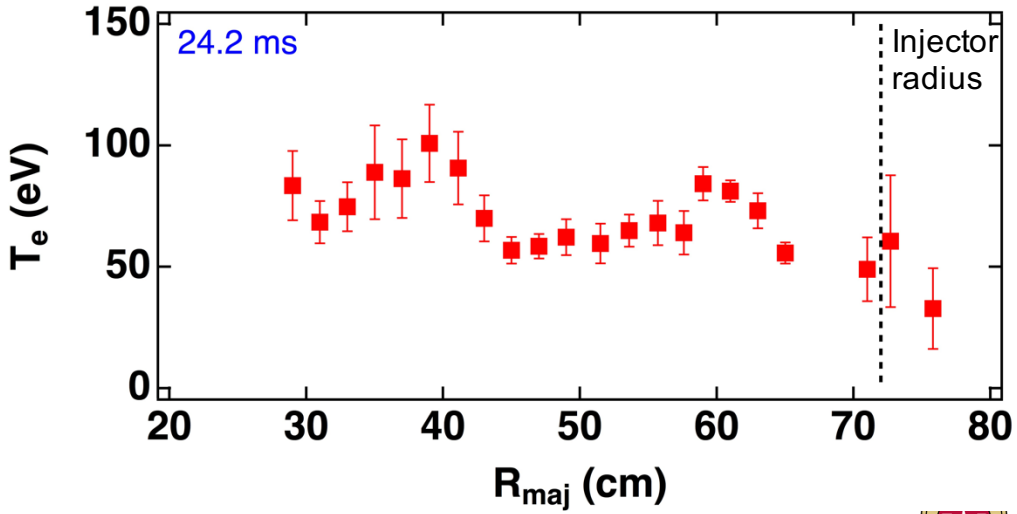


* D.J. Battaglia, et al., Phys. Rev. Lett. **102**, 225003 (2009)

Initial results from LHI plasmas highlight dynamic T_e evolution

- Plasma centroid evolves inward
  - 3 injectors located on outboard side below midplane
- LHI plasmas typically lower density than Ohmic
  - $\langle n_e \rangle \sim 5 \times 10^{18}$ m^{-3}
  - Ensemble average Thomson data to increase SNR *(prior to fast shutter implementation)*
- T_e profiles reveal dynamic evolution:
  - t = 22.2 ms: peaked core T_e, cool injector region
    plasma strongly coupled to outboard drive

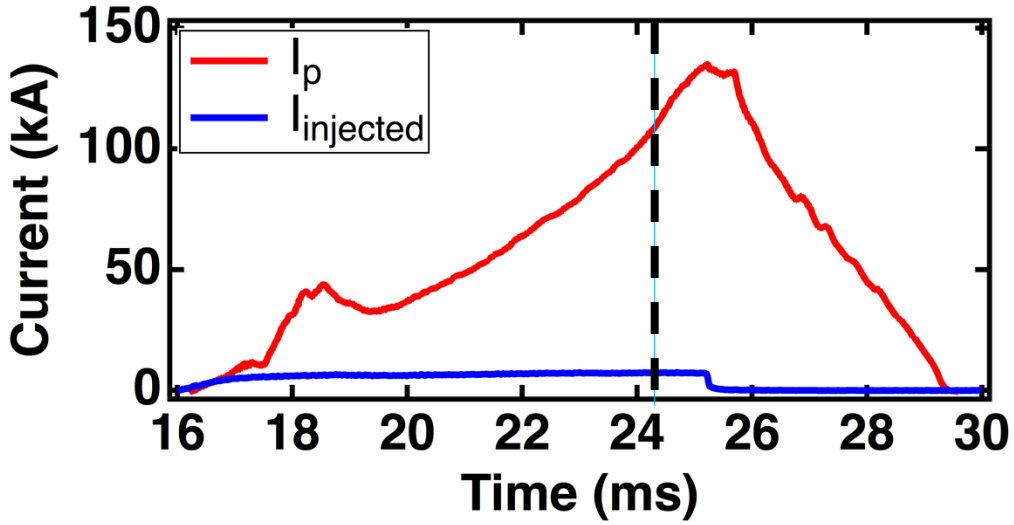


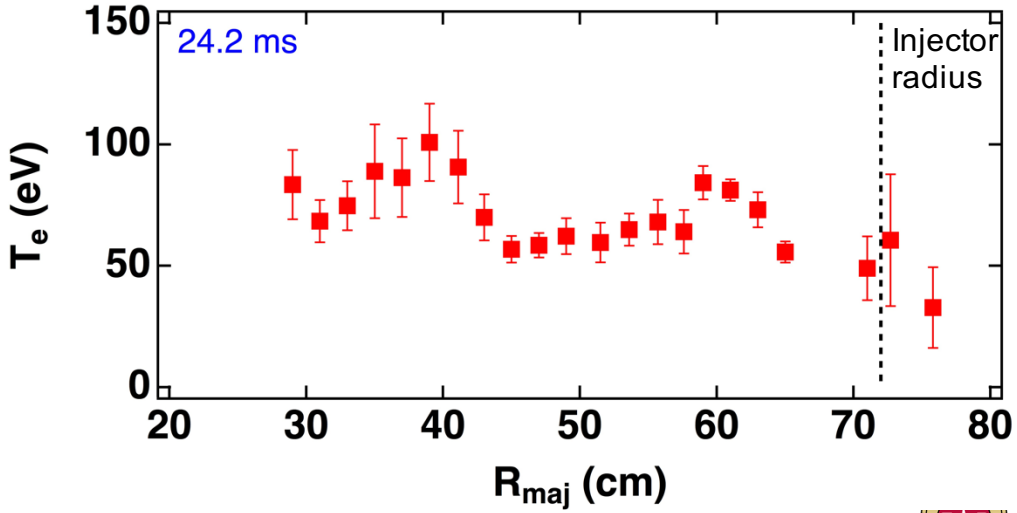


* D.J. Battaglia, et al., Phys. Rev. Lett. **102**, 225003 (2009)

Initial results from LHI plasmas highlight dynamic T_e evolution

- Plasma centroid evolves inward
  - 3 injectors located on outboard side below midplane
- LHI plasmas typically lower density than Ohmic
  - $\langle n_e \rangle \sim 5 \times 10^{18}$ m^{-3}
  - Ensemble average Thomson data to increase SNR *(prior to fast shutter implementation)*
- T_e profiles reveal dynamic evolution:
  - t = 22.2 ms: peaked core T_e, cool injector region plasma strongly coupled to outboard drive
  - t = 24.2 ms: flattened $T_e(R)$, possible internal mode plasma decoupled, decreased drive

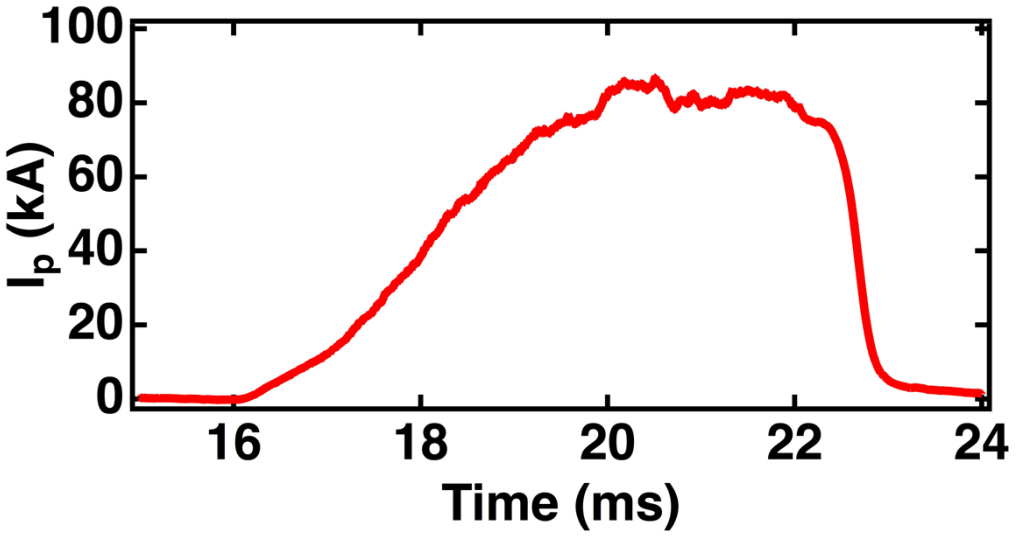


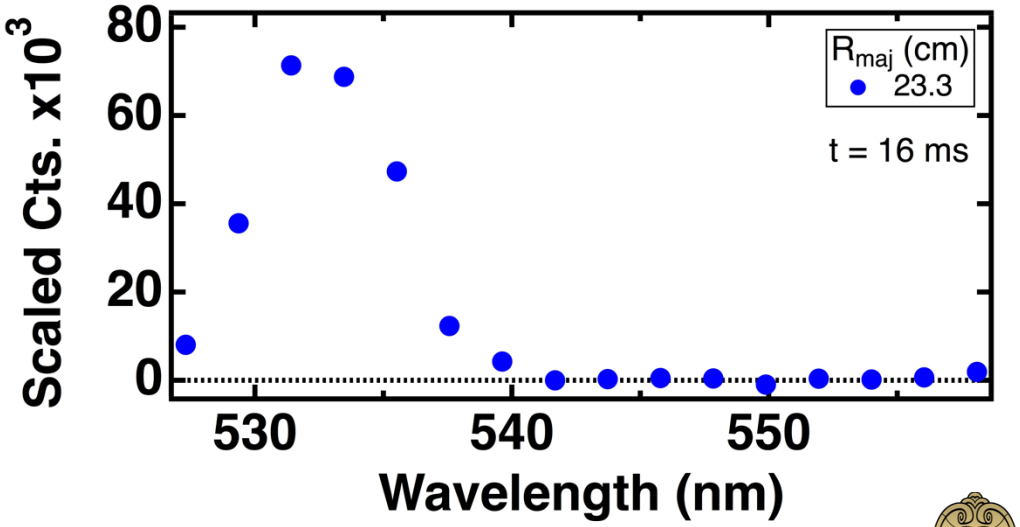


* D.J. Battaglia, et al., Phys. Rev. Lett. **102**, 225003 (2009)

Using full complement of SNR enhancements, single-shot $T_e(R,t)$ achievable

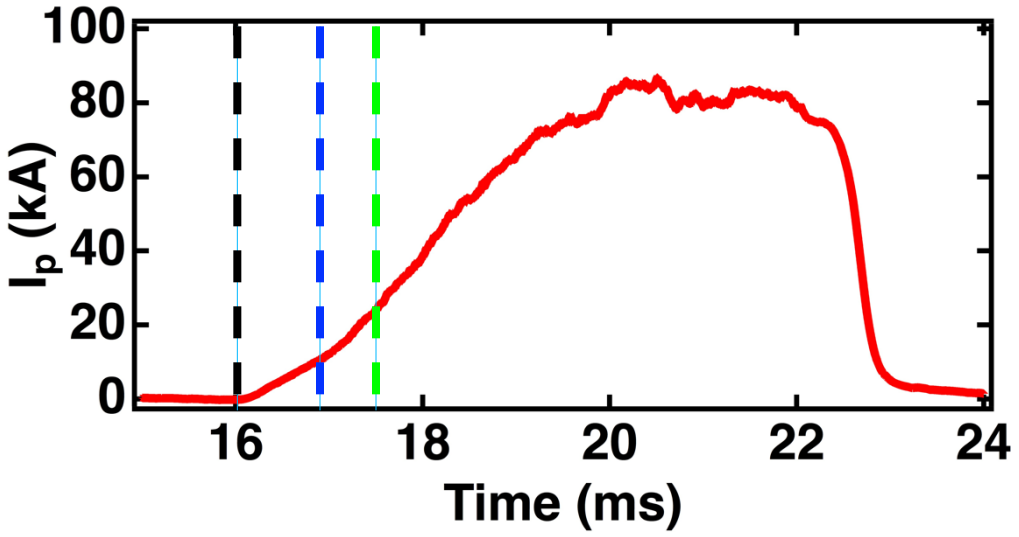
- Physics investigation of low-density startup phase of LHI plasmas
  - $\langle n_e \rangle < 5 \times 10^{18}\ m^{-3}$
- Processed data exhibits clear Gaussian for single-shot measurements
  - Good confidence in calculated temperatures

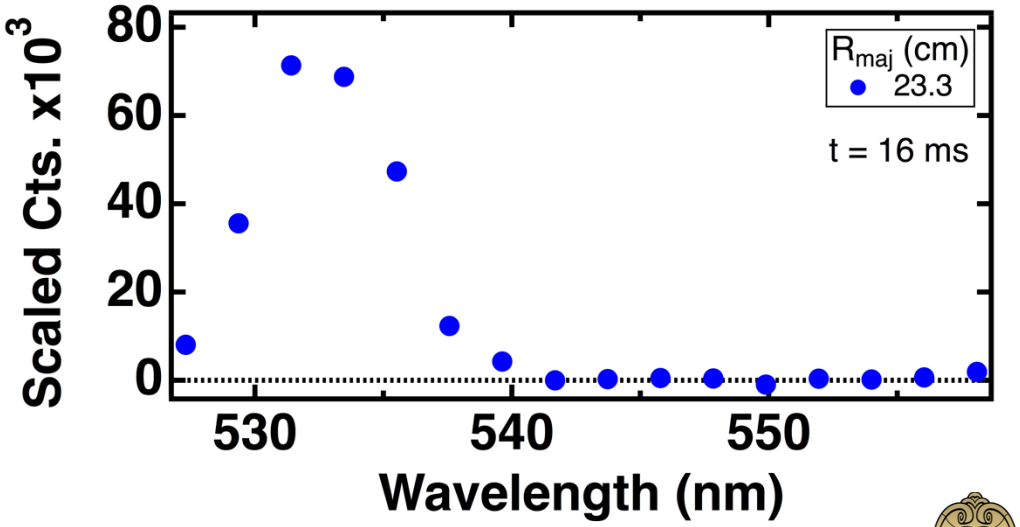




Using full complement of SNR enhancements, single-shot $T_e(R,t)$ achievable

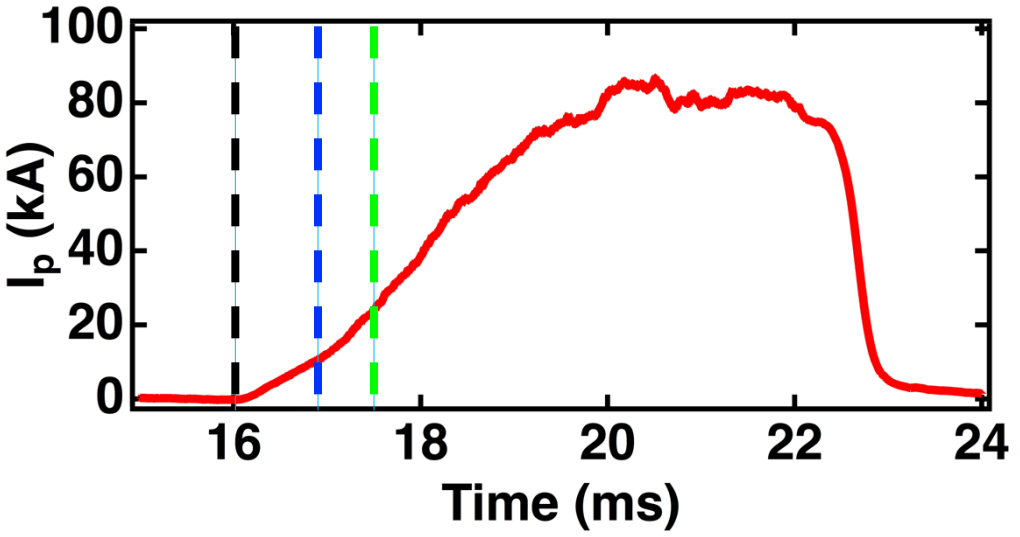
- Physics investigation of low-density startup phase of LHI plasmas
  - $\langle n_e \rangle < 5 \times 10^{18}\ m^{-3}$
- Processed data exhibits clear Gaussian for single-shot measurements
  - Good confidence in calculated temperatures
- $T_e(R_{maj})$ increases rapidly

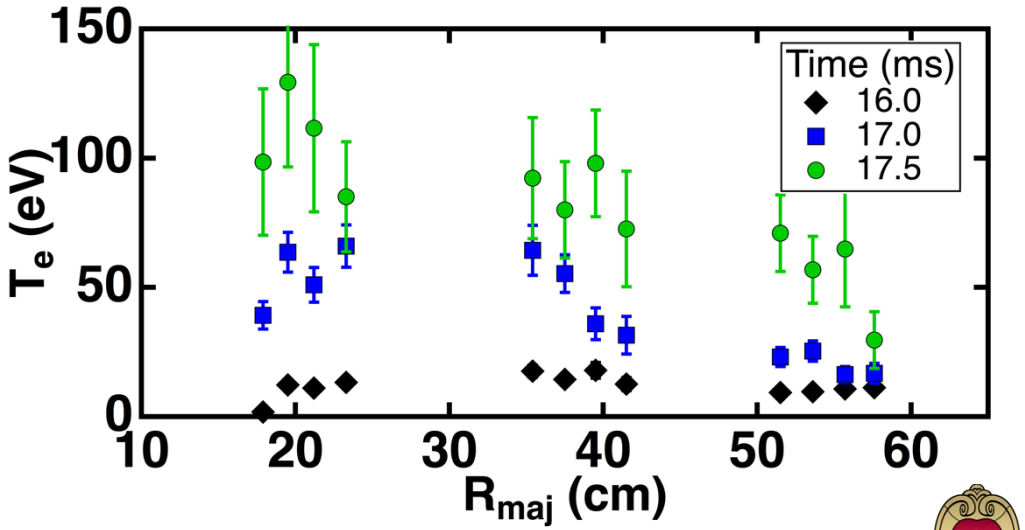




Using full complement of SNR enhancements, single-shot $T_e(R,t)$ achievable

- Physics investigation of low-density startup phase of LHI plasmas
  - $\langle n_e \rangle < 5 \times 10^{18}\ m^{-3}$
- Processed data exhibits clear Gaussian for single-shot measurements
  - Good confidence in calculated temperatures
- $T_e(R_{maj})$ increases rapidly





A novel, high-throughput, optimized Thomson diagnostic is implemented on the Pegasus Toroidal Experiment

- Unique design features include:
  - Time-of-flight stray light rejection
  - Compact, cost-efficient spectrometers
  - Built-in digitization on ICCDs
  - Fast optical shuttering blocks background light

- Next steps:
  - Exchange background channels for data channels
  - Begin characterizing densities during LHI operations



